Engineering and Technology Journal
Journal homepage: https://etj.uotechnology.edu.iq

Design and analysis of reconfigurable filters employing varactor and PIN diodes

Salah O. Mahdi [a*], **Mithaq N. Raheema** [b], **Raaed T. Hammed** [a]

[a] Electrical Engineering Dept., University of Technology-Iraq, Alsina'a street, 10066 Baghdad, Iraq.
[b] Prosthetics and Orthotics Engineering Dept., College of Engineering, University of Kerbala, Kerbala, Iraq.
*Corresponding author Email: eee.20.13@grad.uotechnology.edu.iq

HIGHLIGHTS

- Microstrip filters were classified by reconfigurability functions and the use of varactors or PIN diodes
- The effects of varactors and PIN diodes on filter performance were investigated
- Two stop filter designs using single and dual grounded stepped impedance resonators were introduced

Keywords:
Reconfigurable
Microstrip
Dual-band
PIN diode
Varactor

ABSTRACT

This work presents a comprehensive and comparative study on reconfigurable/tunable microstrip filters, aiming to analyze and understand the impact of varactors, PIN diodes, lumped capacitors, and inductors on the overall filter performance. The study begins by thoroughly classifying reconfigurable microstrip filters based on their reconfigurability functions and the utilization of varactors or PIN diodes. The investigation delves into the influence of varactors and PIN diodes on the performance parameters of microstrip filters. The analysis includes key aspects like center frequency tunability, bandwidth adjustment, and signal attenuation. Additionally, the impact of these reconfigurable elements on insertion loss and return loss is studied to provide a holistic understanding of their role in filter design. Furthermore, the research investigates the interaction between capacitors and inductors in conjunction with varactors and PIN diodes, aiming to clarify their combined effects on filter characteristics. The study involves theoretical modeling and practical experimentation to validate the proposed concepts and results by offering two band stop filters. Accordingly, the first design was implemented to operate at a frequency of 2.4 GHz. In contrast, the second filter involves the realization of two distinct frequencies: an odd-mode frequency of 3.5 GHz and an even-mode frequency of 2.4 GHz. The outcomes of this research are to provide useful insights and guidelines for RF engineers and researchers involved in developing reconfigurable/tunable microstrip filters.

1. Introduction

The expanding requirements in modern wireless communication systems have powered microstrip reconfigurable filter design development. Reconfigurable filters have many improvements, such as flexibility, adaptability, and reduced size and cost. These filters are normally used in wireless communication systems, such as 4G/5G, radar, and satellite systems. They represent important components in adjusting the system performance for dynamic frequency conditions and have been developed to be essential elements in contemporary communication systems. There are several categories of reconfigurable/tunable filters based on reconfigurability and tuning of components. Some adjustable parameters of reconfigurable filters are center frequency, bandwidth, and notch band location. On the other hand, some familiar tuning components include varactor diodes, PIN diodes, and MEMS switches. PIN and varactor diodes are the most common elements for adjusting circuit performance since they are simple to integrate, have low power consumption, and work at high-frequency bands. Varactor diodes behave as voltage-controlled capacitors, whose capacitance value changes based on the applied reverse bias voltage. Varactor diodes tune the filter's response by adjusting the reverse voltage across the varactor diode over a specified range of capacitance values [1].

On the other hand, PIN diodes are operated as current-controlled switches, where their resistance value varies with the forward bias current. PIN diodes operate as high-frequency switches in reconfigurable filters, switching between ON and OFF states with forward and reverse bias voltages [2]. Inductors and capacitors are the essential elements of reconfigurable filter design to control the passband filter characteristics. The operation of inductors and capacitors can be impacted by many

http://doi.org/10.30684/etj.2024.149010.1738
Received 21 April 2024; Received in revised form 25 July 2024; Accepted 29 August 2024; Available online 30 October 2024
2412-0758/University of Technology-Iraq, Baghdad, Iraq

parameters, including temperature, mutual coupling, and manufacturing tolerance. These parameters can affect the insertion loss, frequency shift, and distortion in the desired performance.

This article introduces a comparative study of reconfigurable filters, concentrating on the effect of PIN and varactor diodes, as well as the lumped inductors and capacitors. This review aims to focus on the requirements of the experimental investigation to show the effectiveness of varactors and PIN diodes on the overall filter response. This study has been established to accomplish some objectives. First, it directs the classification of the reconfigurable filter into separate groups according to the functions of the reconfigurability process and the use of varactors or PIN diodes. Also, the paper aims to investigate the effects of reconfiguring elements on filter performance, including bandwidth, center frequency, return loss, and insertion loss. Confirmed by theoretical demonstration and practical investigation, this study offers a detailed review of the utilization of varactors, PIN diodes, inductors, and capacitors in reconfigurable filter design.

2. Classification of reconfigurable and tunable filters

Reconfigurable filters can be classified into several categories according to the performance parameters to be adjusted. The following subsections illustrate several reconfigurable/tunable filters classified based on passband type, center frequency shift, bandwidth adjustment, and notch band location. Comparison tables have been given to identify the distinctive characteristics of different approaches in numerous works concentrated on reconfigurable/tunable filter design.

2.1 Microstrip filters with reconfigurable passbands

PIN diode switches can be used to change the filter type. Switching on or off some PIN diodes connected to certain stubs in the filter structure can alter the passband or stop-band regions, resulting in different filter types. A recorded method involves using a microstrip filter structure that can change between bandstop and band-pass performance using square ring resonators and open-circuited stub resonators [3]. The design of the filter structure is tailored to achieve optimal performance at a specific frequency, which in this case is 11.2 to 14.5 GHz. RF-PIN diodes from Skyworks (HMPP3890) were used to perform the reconfigurability function [3]. In another study, the authors present a novel model of a compact reconfigurable low-pass/band-pass filter constructed on a metamaterial transmission line. Reconfigurability is achieved by incorporating switches in the cells, allowing for operation in band-pass mode when all reconfiguring switches are in the ON state and low pass mode when switch 1 is in the OFF state and switch 2 is in the ON state.

The proposed low-pass filter has a 3-dB cutoff frequency at 3.25 GHz. On the other hand, the band-pass filter is centered at 3.65 GHz, exhibiting a matched bandwidth with S_{21} of -0.2 dB [4]. Another work introduces a new compact reconfigurable planar low pass/band pass filter designed for 5G applications, operating at 0 - 1 GHz and 3.4 - 3.8 GHz frequency bands. Adding a fourth resonator between the input and output ports assists the achievement of low-pass characteristics and improves the system's reconfigurability [5]. In another article, the authors present a loop-shaped filter capable of applying the reconfigurability technique [6]. The designed filter performs as a band-stop or band-pass filter by incorporating the resonator into the transmission line that connects the source and load. Two BAR64-03 PIN switches with a series resistance of 2.1 Ω, an inductance of 1.8 nH in the ON state condition and 3 kΩ reverse resistance, and 0.17 pF shunt capacitance in the OFF condition are used to model the PIN diodes. Li et al. [6] developed a reconfigurable filter functioning at 1.5, and 1.6 GHz to validate the concept. The RF signal and DC lines are isolated by an RF choke inductor of 47 nH and a DC-blocking capacitor of 18 pF. Another work introduces two reconfigurable band stop/band-pass filters operating in the C and X bands. The reconfigurability is accomplished by utilizing semiconductor-distributed doped areas. The filter design considered two frequencies of 5 GHz and 10 GHz [7]. Another proposed novel design introduces a dual wide-band filter, which can switch between band stop/band-pass filters using PIN switches. The design utilizes an open loop resonator, and by incorporating PIN diodes and vias, it can function as both a band pass/band stop filter. The bandstop filter operates in the frequencies of (1.3, 3.2) GHz, and (5.6, and 7.5) GHz, corresponding to the S-band and C bands [8]. Table 1 presents a summarized comparison of the mentioned works above.

Table 1: Comparative performance analysis of previous microstrip filters with reconfigurable passbands studies

Reconfigurability Function	Frequency band-pass (GHz)	B.W (%)	Frequency stop band (GHz)	B.W (%)	S_{11} $(-dB)$	S_{21} $(-dB)$	Circuit size $(\lambda_g \times \lambda_g)$	No. of reconfiguring elements	Ref.
BPF/BSF single wide band	8.5–14, 9 – 15.5	47.82, 54.16	9–15.5, 8.5 – 14	54, 48	20 1.2	1.6 30	0.9 × 0.96	4	**[3]**
Narrow, Wide BPF/LPF	3.6	55	-	-	20	0.6	0.2 × 0.22	7	**[4]**
BPF/LPF	0–1, 3.4–3.8	100, 11	-	-	30	1.4	0.4 × 0.32	1	**[5]**
BPF/BSF	1.5, 1.6	7	1.5, 1.6	7	23 2.3	1.3 18	0.27 × 0.12	2	**[6]**
BPF/BSF	5, 10	70	5, 10	70	50 2.1	2.6 30	0.32 × 0.35	2	**[7]**
BPF/BSF Dual Band	1.3–3.2, 6.5 - 7.5	84, 8	1.3–3.2, 6.5 - 7.5	85, 7	42 0.6	0.9 35	0.45 × 0.45	2	**[8]**

2.2 Reconfigurable wide-band filters with narrow notch bands

Among these techniques, a reconfigurable ultra-wideband antenna with tri-band notched responses was considered. The notched bands are achieved using a band stop filter with a defected microstrip structure and an inverted-shaped slot. The filter operates over a frequency range from 3.1 to 14 GHz with three band notches at 4.2–6.2 GHz, 6.6–7.0 GHz, and 12.2–14 GHz. The reconfigurable characteristics are accomplished by integrating four diodes [9]. Another approach introduces a new reconfigurable filtering antenna for modern wireless techniques. The feeding line of the antenna is made up of a stepped-impedance resonator. Incorporating MA4AGBLP912 PIN switches enables the filter to switch between an ultra-wideband and a dual bands state. The filter works at 3.35 GHz and 5.2 GHz center frequencies in the dual-band situation. An inductor of 30-nH and a capacitor of 2.2 pF are attached by stepped impedance resonators and microstrip lines to constitute the DC biasing circuit [10]. Moreover, another article studies design approaches for band-pass filters with reconfigurable characteristics suitable to modern communication applications, including the (3.4–3.77 GHz) band. The focus is on achieving regulation for parameters such as frequency, bandwidth, and selectivity, even decreasing the need for numerous reconfiguring components between electrical elements [11].

A different work explores a reconfigurable dual-functional filter designed for wide-band and tri-band pass filter applications. The wide band structure is achieved by constructing short-circuited and open stub-loaded resonators, providing a passband from 2 GHz to 6.1 GHz. The triple band-pass filter offers 2.4, 3.5, and 5.2 GHz pass bands. SMP1340–079LF PIN effectively changes the function between wide-band and triple-band modes. The design behavior is investigated through even and odd mode analysis. The DC biasing voltage is provided to the PIN switch via an RF choke inductor of 27 nH, and a 47 pF capacitor is employed for DC blocking [12]. Table 2 describes a summarized comparison of the researches above.

Table 2: Comparative performance analysis of previous reconfigurable wide-band filters with narrow notch-bands studies

Reconfigurability Function	Frequency band-pass (GHz)	B.W (%)	Frequency stop band (GHz)	B.W (%)	S_{11} (−dB)	S_{21} (−dB)	Circuit size ($\lambda_g \times \lambda_g$)	No. of reconfiguring elements	Ref.
BPF with 3-notch bands	3.1-14	127	4.2–6.2, 6.6–7.0, 12.2–14	39, 6, 14	15, 25, 20	1, 0.6, 0.3	0.43 × 0.46	3	[9]
Wideband/dual-band BPF	3.35, 5.2	114, 30, 15	-	-	20	2.3	0.56 × 0.42	3	[10]
BPF	3.4, 3.77	14	-	-	22	1.5	0.51 × 0.51	2	[11]
Wide-band / Triple-band BPF	2 - 6.1, 2.4, 3.5, 5.2	104, 10, 11, 3	-	-	17, 35, 42, 27, 28	1.7, 1.5, 1.1,1.4, 0.9	0.53 × 0.55	10	[12]

2.3 Microstrip filters with reconfigurable center frequency and bandwidth

In another method, the author suggests a comprehensive integration approach for proposing reconfigurable filters with adaptable center frequency and bandwidth response performances for 2.4 GHz frequency, including frequency tuning, bandwidth regulating, and band-pass to bandstop reconfiguration by using PIN and varactor switches [13]. In a separate endeavor, a simple method is presented to design multi-bandpass reconfigurable filters with independent control over center frequency and bandwidth for frequencies from 0.6 to 2 GHz using varactor diodes. The proposed filters can be compounded to form wider transmission bands and operate similarly to ultra-wideband filters with adaptable in-band frequency notches [14]. Furthermore, another study presents a novel design for an ultra-wideband band-pass filter, utilizing square ring resonators combined with an open-tuning L-shaped stub. The benefit of this design lies in its ability to tune the frequency and reconfigure the bandwidth of the dual-band response. The reconfiguration is achieved by fixing SMV1405 varactor diodes on the stub in the microstrip band-pass filter. The response of S_{21} shows fluctuations between -4 and -1.5 dB within the frequency bands 8.3–13.9 GHz, 4.6–6.2 GHz with S_{21} between -0.67 and -0.56 dB, with a variable DC biasing voltage between 30–0 V [15]. Another method involves using the RF design of reconfigurable single and multi-pass band filters and duplexers for 1.24-1.64 GHz and 1.4-1.6 GHz frequencies. The reconfiguration abilities consist of bandwidth tuning and center frequency [16]. Another paper offers a new wide band-pass reconfigurable filter with center frequency reconfiguration. The suggested pass band design connects reconfigurable low-pass and high-pass filter sectors using SMV1405-079LF varactor switches. The measured results show that the filter bandwidth is adjusted from 0.18 to 1.39 GHz at the same center frequency.

Center frequency is correspondingly demonstrated with diverse overall bandwidths of 0.4, 0.6, and 0.8 GHz [17]. In another research, the author outlines the structure and operation of a bandwidth and frequency reconfigurable design within frequencies of 2 GHz to 3 GHz. A total of six switches, two BAR64-03W PIN diode switches, and four SMV2023 varactor switches are utilized in the proposed design. Varactor switches consuming resistance of 1.6 Ω and inductance of 1.5 nH regulate the process. The varactor diodes have a capacitance of 12.33 pF to 1.09 pF, supporting the desired tuning range. PIN diode switches were used for the filter design. Having forward resistance of 2.1 Ω, inductance of 1.8 nH in the ON condition, and reverse resistance of 3 kΩ, with 0.17 pF junction capacitance in the OFF condition. The reconfiguration process is achieved through two PIN diodes, enabling switching between frequency and bandwidth adjustments. For bandwidth tuning, varactor diodes adjust two transmission zeros individually, providing flexibility in reconfiguring the pass edges. An inductor of 33 nH was used as an RF choke, and a DC blocking capacitor of 20 pF was utilized to separate the RF and DC signals [18]. Furthermore, other authors propose a new single-ended-to-balanced (SETB) filter with integrated controllable operating modes between two SETB filters. The circuit is designed to have reconfigurable abilities, containing switchable frequencies, bandwidths, and changeable single/dual band processes using MA46H202 Varactors diode tuned for dual-band design at 500,

600, and 700 MHz and dual-band SETB at 1200, 1300, and 1400 MHz [19]. Table 3 presents a reviewed comparison of the above studies.

Table 3: Comparative performance analysis of previous microstrip filters with reconfigurable center frequency and bandwidth studies

Reconfigurability Function	Frequency band-pass (GHz)	B.W (%)	Frequency stop band (GHz)	B.W (%)	S_{11} $(-dB)$	S_{21} $(-dB)$	Circuit size $(\lambda_g \times \lambda_g)$	No. of reconfiguring elements	Ref.
Frequency and bandwidth BPF	2.4	42	-	-	20	1.2	0.52 × 0.67	3	[13]
Frequency and bandwidth BPF	0.6 - 2	17, 13	-	-	34	0.6	0.75 × 0.98	9	[14]
Frequency and bandwidth BPF	8.327 - 13.942, 4.62 - 6.2	51, 29	-	-	32	0.6	0.66 × 0.66	4	[15]
Frequency and bandwidth BPF	1.24-1.64, 1.4-1.6	28, 13	-	-	42, 40	1.3, 1.7	0.59 × 0.96	4	[16]
Frequency and bandwidth BPF	0.8 – 1.95	12, 83	-	-	20	1.3	0.23 × 0.14	3	[17]
Frequency and bandwidth BPF	2, 3	27, 13	-	-	22	1.5	0.52× 0.67	6	[18]
Frequency and bandwidth BPF	0.5, 1.2	6, 11	-	-	34	2.6	0.17 × 0.27	3	[19]

2.4 Reconfigurable/tunable frequency response filter

A straightforward reconfigurable band-pass filter with the capability to switch between 2.4 and 5 GHz frequencies using BAR88-02V PIN diodes. The electrical length of the open-circuited stubs can be altered between quarter and half wave states by controlling the PIN diodes, thereby tuning the filter's center frequency. Simulated and measured performance demonstrates the filter's states with a broad regulating range of 2.4 GHz to 5 GHz and a band rejection exceeding 40 dB. The presented design used two 22 pF capacitors positioned at the input and output of the design [20]. In another instance, a reconfigurable Band-pass Filter featuring a PIN switch structure is designed to exhibit excellent return loss and band-pass characteristics for wireless communications. It is engineered to work at two distinct frequencies, namely 1.75 and 3.5 GHz, separately by regulatory the switching states of the SKY13351378LF PIN (GaAs SPDT diodes). The filter design aims to provide a fractional bandwidth of 11% at 3.5 GHz and 13% at 1.75 GHz. Three 100 pF capacitors are assigned to the DC biasing network [21]. In another study, the authors introduce a novel approach to designing reconfigurable multiband filters using a memristor-based multilayer dual-mode resonator for 1.6 and 3.5 GHz. The memristor is utilized as an RF regulator element.

The memristor is designed with a 1.37 fF capacitor in OFF condition and a 3.6-ohm resistor in ON condition, enabling a dual band-pass filter with flexible operating modes. The RF choke is designed as an inductor of 30 nH [22]. Additionally, it introduces a new reconfigurable filter designed for versatility in multiple wireless communication systems. BAR64 PIN switches are strategically placed to accomplish multiband reconfigurability techniques spanning between 1.2 and 3.2 GHz, catering to diverse communication frequency requirements.

The DC biasing is separated by a capacitor of 20 pF DC blocking and an RF choke inductor of 33 nH [23]. Another research offers a compact, wide-band, and reconfigurable band-pass filter featuring a circular-shaped multi-mode resonator (MMR). In the OFF condition of the PIN diode, the frequencies are 2.4 GHz, 3.5 GHz, and 5.9 GHz. In the ON state of the PIN state, the filter provides additional center frequencies of 6.5 and 8.8 GHz [24]. In a separate endeavor, a compact and reconfigurable tri-band filter is characterized by controlled passbands and high selectivity. The filter design features six varactors, SMV1405 and SMV2020, inserted in λ/4 short-circuited resonators, allowing for individually tuning each passband by adjusting the voltage attached to the resonators. The three band-passes of the filter show tuning extends from 0.8 to 1 GHz, 1.35 to 1.55 GHz, and 1.8 to 2.02 GHz, respectively. DC block capacitors are 2.2 pF, 1.2 pF, and 0.8 pF. Furthermore, the RF choke inductor is 100 nH [25]. Another study presents a new structure for a reconfigurable dual-band stop filter for the tuning extends from the lower and upper band stop at 1.16 to 1.29 GHz and 1.6 to 1.76 GHz. The biasing network for (θL1, ZL1) contains a 3.6 nH inductor and two 3 pF shunt capacitors. Also, the biasing network for (θL2, ZL2) contains a 1.4 nH inductor and two 2 pF shunt capacitors [26]. Another work introduces a reconfigurable band pass filter (BPF) mounted on a flexible Kapton substrate.

The flexibility and conformability of electronic elements are essential for arranging non-planar components and wearable applications. The frequency reconfigurability in this design is achieved through a switch made of Vanadium Dioxide (VO_2), a Metal Insulator Transition (MIT) material. The VO_2 switch, placed with custom ink, is in the OFF state (operating) at room temperature and changes to the ON state at the MIT temperature of 68 °C. The band-pass filter utilizes dual-mode resonators and changes its operating frequency from 4 to 3.7 GHz. Vanadium Dioxide (VO_2) constructed switch on a flexible substrate. ON state with 5 **Ω** and an OFF state with 1.5 k**Ω**. The needed thermal bias is offered through an installed heater combined with the backside of the designed filter [27]. Besides, a new design reconfigurable dual wide band-pass filters using a fixed frequency and manageable bandstop for 3.5 GHz. Two PIN switches are then employed to reconfigure components, enabling the achievement of three different bandwidth situations. Two RF chokes are utilized [28]. However, another article offers the filter design of a reconfigurable balanced dual band-pass for frequency tuning extending from 2.5 to 3 GHz and 3.3 to 3.8 GHz. Four varactor switches are utilized for reconfigurability with minimal insertion losses [29].

Consequently, another research suggests the model of a reconfigurable pass band filter for wireless communication techniques, specifically addressing the need to reject signals at MHz ranges. The filter utilizes a varactor diode tuning mechanism to achieve electronic tunability. The designed and simulated band-pass filter operates at 1.2 GHz. Tunability is

accomplished by varying the biasing voltage of 0V to 9V applied to the varactor switch. The tuning range spans from 1 GHz to 1.4 GHz. Five capacitors are utilized as DC blocking [30]. In addition, another research is structured into two parts. In the first section, the authors propose a Substrate Integrated Waveguide and half-mode (HMSIW) band-pass filters (BPFs) constructed on balancing hexagonal metamaterial cells. Additionally, the tunable HMSIW band-pass filter is examined and optimized. Two PIN diodes are altered in the frequency band 5.8 to 6.8 GHz. Correspondingly, switching both diodes ON allows a dual-band with two frequencies at 5.6 GHz and 7.4 GHz [31].

The authors propose a new substrate-integrated waveguide reconfigurable band-pass filter in another paper. The design incorporates two different-sized complementary split-ring resonators and two PIN diodes for compact size and reconfigurability. The filter operates in three different modes based on the ON/OFF conditions of the PIN switches. The dual band-pass filter works with a frequency band of 2.5–3.6 GHz, exhibiting measured S_{11} of -23 dB and -25 dB. Alternatively, it can activate as a single band-pass filter (BPF) in two different states: one with a resonant frequency of 2.6 GHz and S_{11} of -20 dB, and the other with a frequency of 3.4 GHz and a measured S_{11} of -35 dB [32].

In a different paper, the authors propose new reconfigurable switches constructed by the evanescent EVA mode cavity for 1.953–2.782 and 1.866–2.257 GHz. The design filter utilizes varactor diodes between two EVA resonators. By directing the MA46H202 varactor switch, the coupling coefficient between resonators can be adjusted to achieve either an OFF or ON condition with a band pass filter response [33]. A different research presents a low-profile triple-notched band stop filter to suppress frequency bands of 2.4, 3.5, and 5.2 GHz. The filter incorporates three MA4AGP907 PIN diodes for reconfigurability, supporting six operating modes. The achieved performance includes S_{21} of -40 dB, -29 dB, and -24 dB, respectively [34]. A reconfigurable triple/quad-band resonator is explained. The filter operates in tri-band or quad-band mode by altering the PIN diode switching state. The operating frequencies corresponding to the band pass filter are 1.2, 2, 2.6, and 3.4 GHz [35]. In other research, a reconfigurable stop band filter designed for multiband application is presented for 2.97, 3.8 GHz operating frequency. The suggested dual stop band filter contains a coupled line between two switchable Capacitively Loaded Loops. Notched bands are adjusted individually by incorporating open circuits as switches in each CLL element [36].

2.5 Microstrip filters with reconfigurable bandwidth

One such technique used a reconfigurable microstrip pass band filter for wireless communication applications, utilizing a dual-mode square loop resonator. The designed filter incorporates two strategically placed MPND4005-B15 PIN diodes as switching elements to achieve switchable bandwidth. The key feature enabling the bandwidth variation is adjusting the length of tuning stubs within the resonator. The filter works at a frequency of 2.4 GHz, and it demonstrates two distinct operational states with different bandwidths. In the first state, the filter achieves a bandwidth of 113 MHz with S_{21} of -1.2 dB. In the second state, the bandwidth is reduced to 35 MHz with a slightly increased S_{21} of -1.5 dB [37]. Also, a novel approach to achieving a compact reconfigurable microstrip band-pass filter with a wide band. The methodology involves varying the spacing, length, and width of transmission lines, enabling the reduction of filter size while improving BW [38]. Similarly, another manuscript presents a compact reconfigurable filter designed for (4G) and (5G) systems. The coupling coefficients between resonators are manipulated to adjust the filter within the 2.5 - 3.8 GHz frequency band. Two SMV1231 varactor diodes and biasing circuit components are selected and designed for the tunable filter. Two (L1 = L2 = 10 nH) inductors are RF chokes [39]. Table 4 presents a comparative performance of the reconfigurable/tunable frequency response filter. While Table 5 represents the comparative performance of the reconfigurable bandwidth filters.

Table 4: Comparative performance analysis of previous reconfigurable / tunable frequency response filter microstrip studies

Reconfigurability Function	Frequency band-pass (GHz)	B.W (%)	Frequency stop band (GHz)	B.W (%)	S_{11} ($-$dB)	S_{21} ($-$dB)	Circuit size ($\lambda_g \times \lambda_g$)	No. of reconfiguring elements	Ref.
Reconfigurable BPF	2.4, 5.2	101	2.4, 5.2	46	20 14	1.3 1.4	0.41 × 0.76	2	**[20]**
Reconfigurable BPF for a Single band	1.75, 3.5	13, 11	-	-	17 41	1.4 1.2	0.86 × 0.31	6	**[21]**
Reconfigurable multiband filters	1.6, 3.5	9, 8	-	-	20, 25	2.6, 3	0.25 × 0.39	2	**[22]**
Reconfigurable multiband BPF	1.2, 1.8, 2.4, 3.2	5, 7, 9, 5	-	-	25, 16, 23, 15	1.5, 1.1, 1.3, 2.1	0.2 × 0.12	3	**[23]**
Reconfigurable multiband BPF	2.43, 3.5, 5.9, 6.5, 8.8	10, 11, 10, 3	-	-	15, 20, 21, 25, 12	0.5, 0.6, 0.7, 1.2, 1.9	0.38 × 0.3	3	**[24]**
Tunable tri-band filter	0.9, 1.4, 1.9	11, 14, 11	-	-	40, 35, 34	3.3, 2.8, 3.2	0.12 × 0.16	3	**[25]**
Dual-band bandstop	-	-	1.2, 1.7	10, 9	1.3, 0.9	20.5, 30.7	0.56 × 0.68	4	**[26]**
Dual-band bandstop	3.8	13	-	-	2.1	20	0.23 × 0.22	3	**[27]**
Reconfigurable multiband BPF Narrow, Wide BPF	3.5	23	-	-	40	2.3	0.69 × 0.52	2	**[28]**

Table 4: Continued

Reconfigurability function	Frequency band-pass (GHz)	B.W (%)	Frequency stop band (GHz)	B.W (%)	S_{11} (−dB)	S_{21} (−dB)	Circuit size ($\lambda_g \times \lambda_g$)	No. of reconfiguring elements	Ref.
Reconfigurable dual-band band-pass	2.7, 3.5	5, 14	-	-	14, 32	1.2.1, 1.6	0.62 × 0.41	4	[29]
Reconfigurable band-pass filter	1.2	17	-	-	47	1.5	0.24 × 0.18	5	[30]
tunable HMSIW band-pass filter	5.8, 6.8	6, 8	-	-	36, 32	0.5, 0.1	0.23 × 0.42	2	[31]
band-pass filter (BPF).	2.5, 3.6	2, 2.3	-	-	23, 25	0.9, 0.8	0.15 × 0.33	2	[32]
reconfigurable single-pole-multi throw (SPMT) switches	1.95–2.78, 1.86–2.25	35, 19	-	-	47, 36, 34	3.1, 2.8, 2.5	0.57 × 0.57	3	[33]
triple-notched band stop filter (BSF)	-	-	2.4, 3.5, 5.2	23, 12, 4	1.2, 1.6, 1.1	40, 29, 24	0.61 × 0.26	3	[34]
reconfigurable tri/quad-band	1.2, 2, 2.6, 3.4	14, 18, 12, 8	-	-	52, 55, 50	1.2, 0.9, 1.6	0.14 × 0.09	2	[35]
reconfigurable band stop filter	-	-	2.97, 3.8	3, 2	15, 17	4, 3.5	0.44 × 0.44	2	[36]

Table 5: Comparative performance analysis of previous microstrip filters with reconfigurable bandwidth studies

Reconfigurability Function	Frequency band-pass (GHz)	B.W (%)	Frequency stop band (GHz)	B.W (%)	$S_{11}(-dB)$	$S_{21}(-dB)$	Circuit size ($\lambda_g \times \lambda_g$)	No. of reconfiguring elements	Ref.
Reconfigurable Narrow, Wide BPF	2.4	2, 5	-	-	27	1.5	0.91 × 0.91	2	[37]
wide band	5.7	26	-	-	14	0.5	0.76 × 0.14		[38]
Tunable Filter	2.5, 3.8	4, 3	-	-	26	2.3	0.35 × 0.21	2	[39]

3. Characteristics of the tuning and reconfiguring elements

A critical aspect of this review is examining tuning elements employed in reconfigurable microstrip filters. Varactors, PIN diodes, capacitors, and inductors, among others, form the building blocks of these filters. The literature surveyed will clarify these elements' roles, individually and in combination, in achieving the desired reconfigurability and performance enhancements. Switches are fundamental components that are responsible for the reconfigurability of the proposed filter design. The switch characteristics completely affect the reconfigurable filter properties. For this purpose, switching techniques are important in the reconfigurable filter design. The reconfigurable filter uses an RF switch to open or close the current path on the filter's surface. By opening and closing switches, the current flow will focus on the required path that changes the filter's response. When there is no applied voltage, the switch will act as an open circuit, but if there is an applied voltage, it will work as a low-impedance line.

Some important characteristics of a switch are [40]:

3.1 Characteristic impedance

This factor estimates how the signals are transmitted or reflected in the transmission line.

3.2 Bandwidth

The operational bandwidth represents the maximum operating frequency for RF switches.

3.3 Topology

Single Pole Double Throw (SPDT) relays and multiplexers are the most important RF switch topologies. SPDT relay connects two inputs to one output or vice versa. The multiplexer is a switching system that directs multiple inputs to a single output or vice versa. It is important to calculate the optimal process for these topologies to choose the required topology in a particular application.

3.4 Insertion loss

This term describes the input-to-output power ratio while the RF switch is on and off. In a specific frequency range, the insertion loss can determine the power loss created by RF diodes on a signal. Equation (1) utilized to evaluate the power loss as follows:

$$\text{Insertion Loss (dB)} = 10\log_{10}\left(\frac{P_{out}}{P_{in}}\right) \quad (1)$$

3.5 Switching speed

Defines the required time for the RF switch to transition from the off to the on state or vice versa. RF switching speeds of the semiconductor switches are usually in the range of nanoseconds, while in the mechanical switches, the switching speeds are in the range of milliseconds.

3.6 Expected lifetime

This step estimates the number of switching transitions before the RF switch fails.

3.7 Power handling

The total power required to operate RF switches is measured in watts. The tuning elements within the framework of reconfigurable microstrip filters serve as essential components, enabling adaptability and responsiveness. These elements are accurately designed to effect alterations in specific characteristics of the filter, thereby ensuring compatibility with varying communication standards, frequency bands, and changing environmental conditions. A comprehensive summary of the various reconfiguring elements utilized in previous research papers is shown in Table 6.

Table 6: Comprehensive summary of the various reconfiguring elements utilized in different papers

Switch model	Frequency band	Features	Ref.
PIN (HMPP3890)	up to 6 GHz	Rs = 2.5 Ω, Cj = 0.3 pF,	[3]
PIN (BAR88)	0.5 to 6 GHz	Rs = 1.5 Ω, Cj = 0.4 pF, Rj = 65k Ω	[4,20]
PIN (BAR64)	1 MHz to 3 GHz	Rs = 2.1 Ω, Cj = 0.17 pF, Rj = 3k Ω	[6,18,23]
PIN (MA4AGBLP912)	up to 40 GHz	Rs = 4 Ω, Cj = 0.028 pF, Rj = 10k Ω	[10,34]
PIN (SMP1340-079LF)	10 MHz to 10 GHz	Rs = 1 Ω, Cj = 0.3 pF, Rj = 65k Ω	[12]
Varactor (SMV1405)	up to 10 GHz	Rs = 0.8 Ω, Ct = 0.62 to 2.67 pF, V bias = 30 to 0 v	[15,17,25,29]
Varactor (SMV2020)	up to 10 GHz.	Rs = 4.1 Ω, Ct = 0.35 to 3.2 pF, V bias = 20 to 0 v	[17,25]
Varactor (SMV2023)	up to 10 GHz.	Rs = 1.6 Ω, Ct = 1.29 to 12.23 pF, V bias = 20 to 0 v	[18]
Varactor (MA46H202)	up to 10 GHz.	Rs = 0.8 Ω, Ct = 2.7 to 3.3 pF, V bias = 20 to 0 v	[19,32]
PIN (SKY13351378LF)	20 MHz to 6.0 GHz	Rs = 0.8 Ω, IL = 0.35 dB, Isolation = 24 dB	[21]
PIN (MADP-000907)	up to 70 GHz	Rs = 5.2 Ω, Cj = 0.025 pF	[28]
Varactor (SMV1231)	beyond 2.5 GHz	Rs = 1.5 Ω, Ct = 0.466 to 2.35 pF, V bias = 15 to 0 v	[30,39]
PIN (MPND4005)	up to 20 GHz	Rs = 6.5 Ω, Cj = 0.02 pF	[37]

To clarify the effect of the reconfiguring elements, this research introduces two basic design techniques for developing a reconfigurable band-stop filter (BSF). These techniques achieve the desired stop bands using single and dual-ground stepped impedance resonators. The studied filter is simulated by Advanced Design System (ADS) software [41]. To justify the design theory, two filters are manufactured and measured: the first filter design performs a center frequency of 2.4 GHz with a bandwidth of 560 MHz, whereas the second filter design includes two stop-bands at 2.4 GHz and 3.5 GHz with bandwidths of 480 MHz and 460 MHz, respectively.

4. Methodology

This section presents two design examples to demonstrate the basic principles of reconfigurable filters. The stepped impedance resonator (SIR) is used as the primary configuration to enhance the rejection band operation of the filter [42,43]. The first filter design serves as a simple case study, exploring the application of a resonator stub or its cancellation via a PIN diode. A dual-mode resonator with two stubs is utilized in the second filter design. Due to the design symmetry of the second configuration, the presented filters are synthesized by the even–odd analysis approach.

In Figure 1 (a and b), the fundamental configuration of the Schematic Diagram for the Stepped Impedance Resonator is presented, illustrating the first filter design. This design incorporates reconfigurability through the application of the SMP-1430-079 PIN diode. The geometry and layout of the resonator highlight the key elements crucial for achieving the desired filter characteristics. The practical circuit provided the required bias supply voltage, RF chokes, and DC-blocking capacitors. When PIN diode D1 is biased in the forward region, the feeding line L_f is loaded in its mid-point by the shorted stub L_p as illustrated in Figure 2 (a). This will produce a dual-mode resonator with two transmission zeros (or two stop-band frequencies). On the other hand, when D1 is biased in the reverse region, the shorted stub will be disconnected from the series feeding line, as shown in Figure 2 (b). In this case, the output signal is the same as the input signal but with some phase shift that depends on the electric length of the series transmission line L_f, assuming that its characteristic impedance Z_f is equal to 50 ohms. It is well known that the series line width. W_f is inversely proportional to the characteristic impedance Z_f, and the width of the parallel stub W_p is inversely proportional to Z_p. The filter structure in Figure 2 (a) is symmetrical and can be analyzed by the odd/even mode theory. The odd mode equivalent circuit is obtained by bisecting the original structure and producing a voltage null (short-circuit) in the middle plane, as illustrated in Figure 3 (a). Conversely, the even mode equivalent circuit is obtained by bisecting the original structure and producing a voltage peak (open-circuit) in the middle plane, as illustrated in Figure 3 (b).

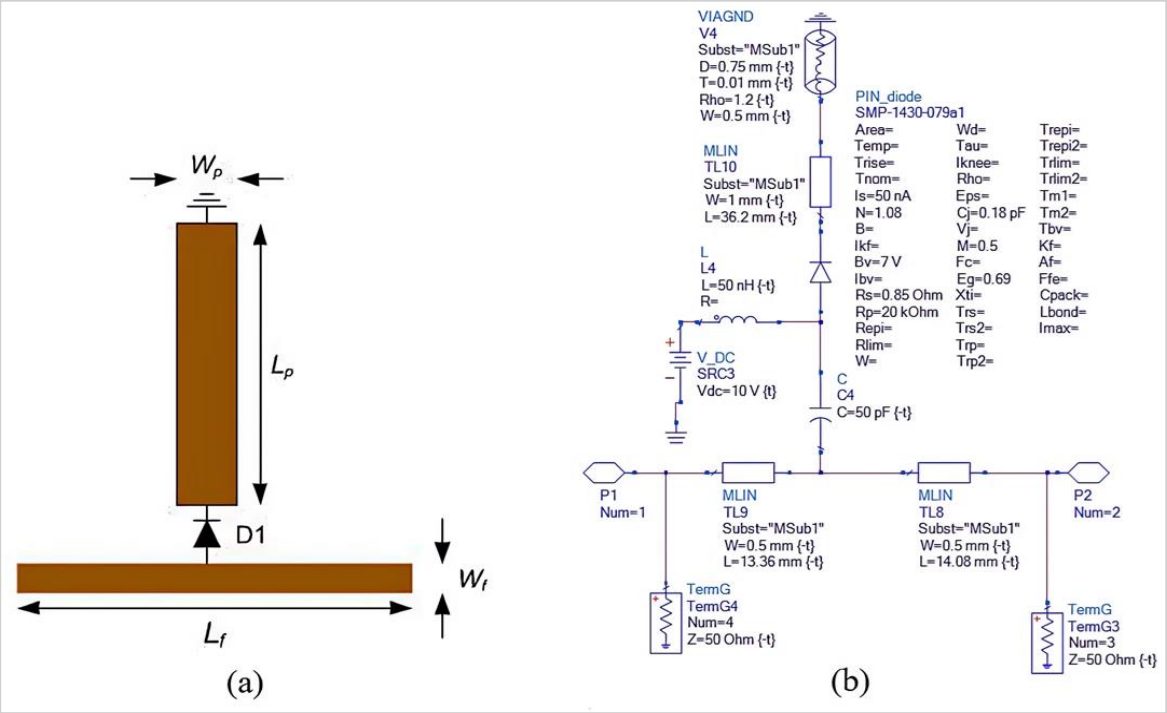

Figure 1: Microstrip bandstop filter with reconfigurable stub employing SMP-1430-079 PIN Diode (Design No. 1) (a) generalized structure (b) schematic diagram

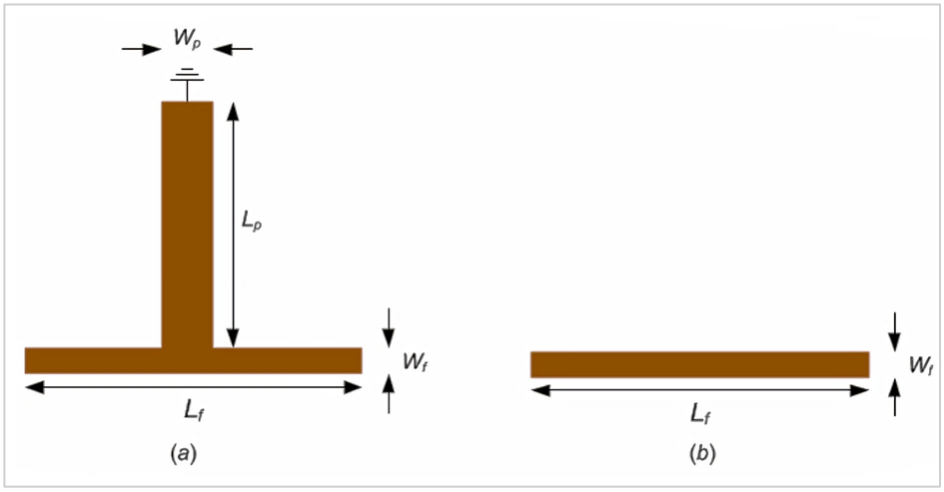

Figure 2: The equivalent structures of the filter when the PIN diode is (a) ON and (b) OFF

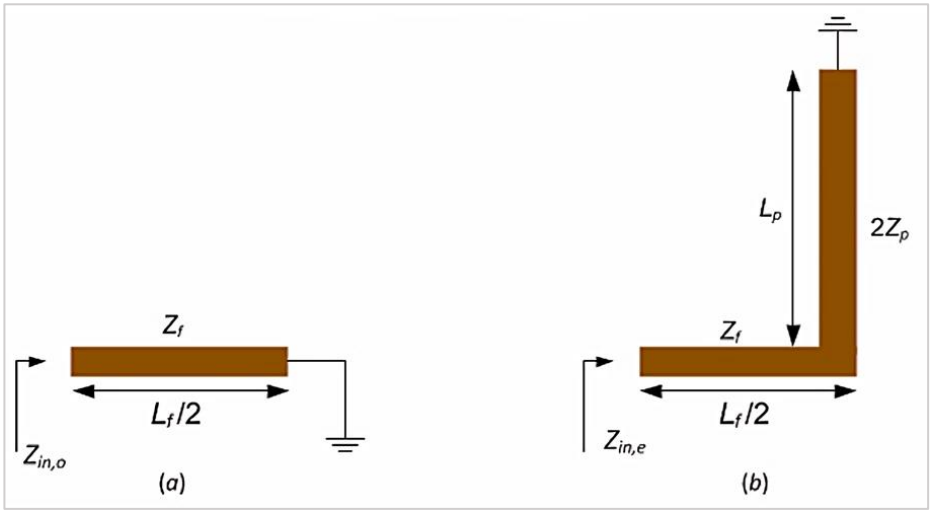

Figure 3: Equivalent circuit structures for the band stop filter when the PIN diode is on (a) odd mode and (b) even-mode

When the structure of Figure 2 (a) is excited, it can be represented by two equivalent circuits. If the dominant mode is the odd mode, the configuration corresponds to a filter operating at a frequency denoted by "f_{odd}" which characterizes the desired upper stop-band frequency. Conversely, if the dominant mode is the even mode, the configuration corresponds to a filter operating at a frequency referred to as "f_{even}", representing the desired lower stop band.

The input impedance for a generalized transmission line is given by:

$$Z_{in} = Z_0 \frac{Z_L + jZ_0 \tan(\beta l)}{Z_0 + jZ_L \tan(\beta l)} \quad (2)$$

For odd-mode analysis, the equivalent circuit is depicted in Figure 3(a), and hence, the odd-mode input impedance according to Equation (2) is expressed by:

$$Z_{in,o} = jZ_f \tan(\beta L_f/2) \quad (3)$$

The frequency at the first transmission zero can be found by equating $Z_{in,o}$ to zero in Equation (3), which implies that:

$$\frac{\beta L_f}{2} = \pi \quad (4)$$

Substituting for β = 2π/ λg and $\lambda_g = c/f\sqrt{\varepsilon_{eff}}$ in Equation (4), the odd-mode frequency which represents the desired upper stop-band is therefore:

$$f_{odd} = \frac{c}{L_f \sqrt{\varepsilon_{eff}}} \quad (5)$$

Equation (5) represent the operating odd frequency. For even-mode analysis, the equivalent circuit is shown in Figure 3(b), and accordingly, the even-mode input impedance is:

$$Z_{in,e} = jZ_f \frac{2Z_p \tan(\beta L_p) + Z_f \tan(\beta L_f/2)}{Z_f - 2Z_p \tan(\beta L_f/2) \tan(\beta L_p)} \quad (6)$$

Now, by equating $Z_{in,e}$ to zero in Equation (6) to produce a second transmission zero, we have:

$$2Z_p \tan(\beta L_p) + Z_f \tan\left(\frac{\beta L_f}{2}\right) = 0 \quad (7)$$

To simplify the analysis, we can assume that Wp = 2Wf, or Zp = Zf/2, and therefore Equation (7) reduces to:

$$\tan(\beta L_p) + \tan\left(\frac{\beta L_f}{2}\right) = 0 \quad (8)$$

Using trigonometric identities to Equation (8), it can be shown that:

$$\beta L_p + \frac{\beta L_f}{2} = \pi \quad (9)$$

Substituting for β = 2π/ λg and $\lambda_g = c/f\sqrt{\varepsilon_{eff}}$ in Equation (9), the even-mode frequency representing the desired lower stop-band is:

$$f_{even} = \frac{c}{(L_f + 2L_p)\sqrt{\varepsilon_{eff}}} \quad (10)$$

where Zo is the characteristic impedance of the transmission line (50 Ω), Z_L is the load impedance, Z_f is the characteristic impedance of the feeding line, Zp is the characteristic impedance of the short-circuited stub, L_f is the length of the feeding transmission line, L_p is the length of the stub, c is the speed of light, and ε_{eff} is the effective permittivity of the microstrip line. Equation (10) represent the operating even frequency. The insertion loss of the filter can be derived in terms of $Z_{in,o}$ and $Z_{in,e}$and is given by Equation (11):

$$S_{21} = \frac{Z_{in,e} \cdot Z_0 - Z_{in,0} \cdot Z_0}{(Z_{in,e} + Z_0) \cdot (Z_{in,0} + Z_0)} \quad (11)$$

where Z_0 = 50 Ω. Moving to Figure 4 (a and b), a detailed depiction of the Schematic Diagram for the dual-mode Stepped Impedance Resonators is presented, representing the second filter design. In this case, reconfigurability is also implemented using an SMP-1430-079 PIN diode. The dual-mode resonator configuration adds a layer of complexity, and the schematic provides insights into how the design achieves its intended performance. Both tuning elements in Figures 1 and 4 are subject to control through dedicated DC biasing circuits. These circuits feature a 50 nH inductor, an RF choke to ensure isolation of the RF signal from the DC supplying circuit, and a 50 pF capacitor, functioning as a DC blocking circuit to prevent the DC signal from walking through the input/output RF ports. The presence of these elements facilitates precise control over the

reconfigurable aspects of the filters, offering a useful means of tuning and adapting the filter response to specific operational requirements. From the information provided earlier, we can draw that the first reconfigurable bandstop filter design is characterized by a single stub resonator strategically implemented to operate at a frequency of 2.4 GHz. The physical construction of this filter involves the fabrication of a grounded substrate with a thickness measuring 0.8 mm.

The substrate chosen for this implementation comprises FR4 material, recognized for its electrical properties, specifically with a relative permittivity denoted as ε_r = 4.3. The details of the proposed filter's specific dimensions, precisely outlined in Table 7, have been methodically determined and are thoroughly illustrated in the accompanying layout diagram, as showcased in Figure 5. This detailed representation not only communicates the structural details of the filter but also underscores the precision of the design process. The resonators of the design experienced a careful photographic etching process, and subsequently, they were assembled to create an organized and integrated circuit. This comprehensive assembly process is brightly depicted in Figure 5, showcasing the steps involved in constructing the combined circuit.

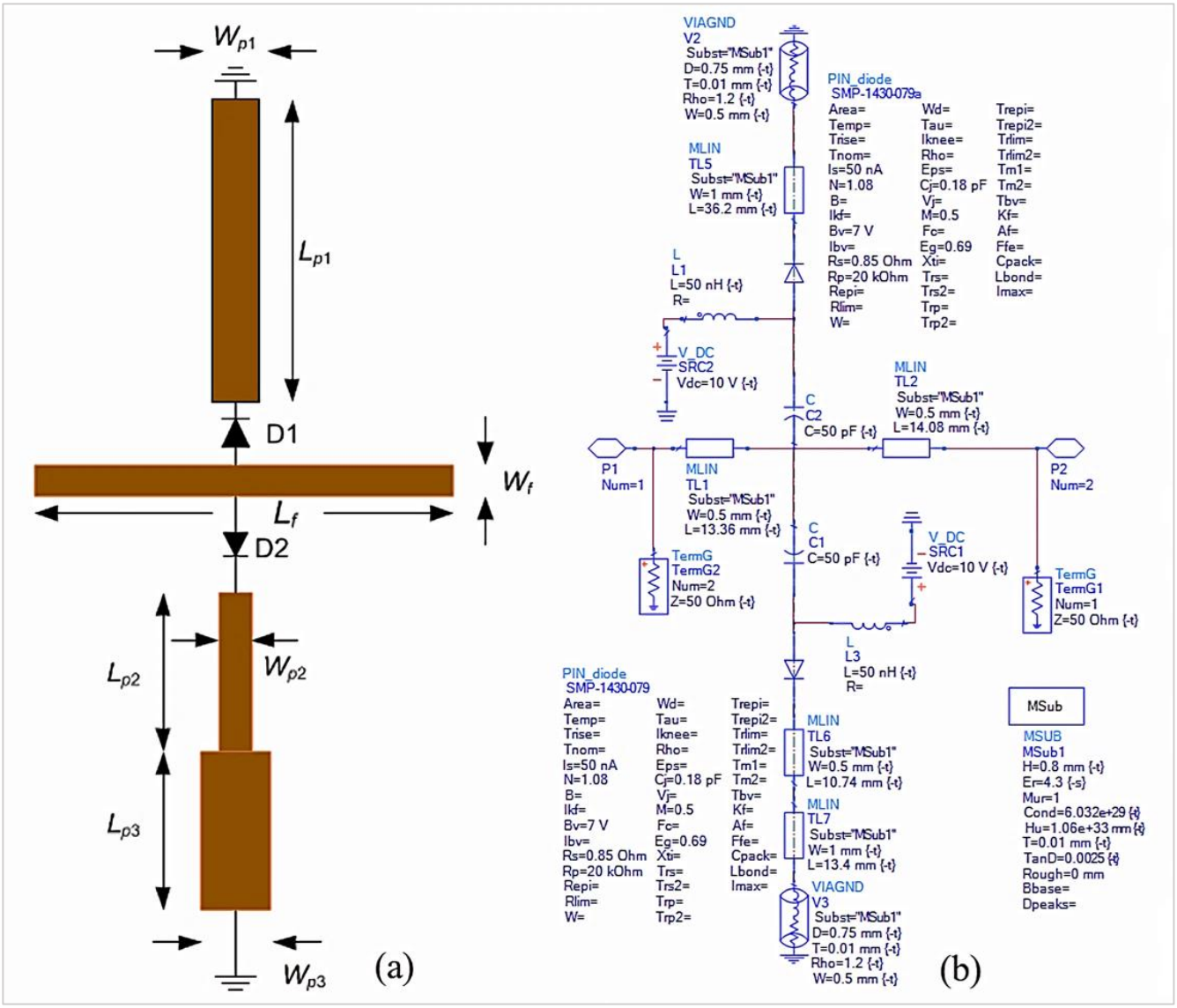

Figure 4: Microstrip bandstop filter with dual reconfigurable stubs utilizing SMP-1430-079 PIN diodes (design no. 2) (a) generalized structure (b) schematic diagram

Table 7: Geometrical dimensions overview for the reconfigurable bandstop filter (design no. 1)

Parameters	h	L_1	L_p	L_f	W_p	W_f
Dimension (mm)	0.8	41	36.2	27.44	1	0.5

In the same fashion, implementing the second reconfigurable dual-mode bandstop filter involves the realization of two distinct frequencies: "f_{odd}" set at 3.5 GHz and "f_{even}" established at 2.4 GHz. This complicated filter structure is accurately structured on a grounded substrate featuring a thickness of 0.8 mm. The chosen substrate material for this design is FR4, which is popular for its dielectric properties and is characterized by a relative permittivity denoted as ε_r = 4.3. The specific dimensions that govern the geometry of this proposed filter are fully detailed in Table 8, providing an insightful understanding of the structural details. These dimensions are considerately presented within the schematic diagram, illustrated in Figure 6.

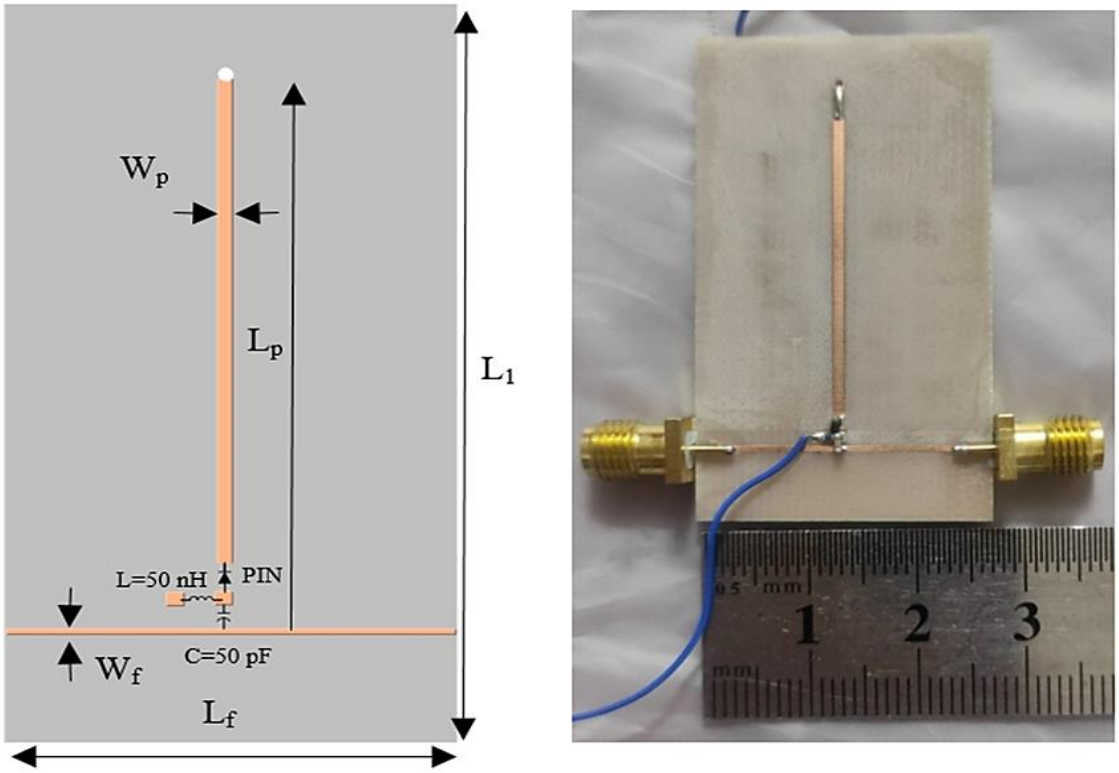

Figure 5: Photograph and layout scheme of the fabricated microstrip bandstop filter with reconfigurable employing SMP-1430-079 PIN diode (design no. 1)

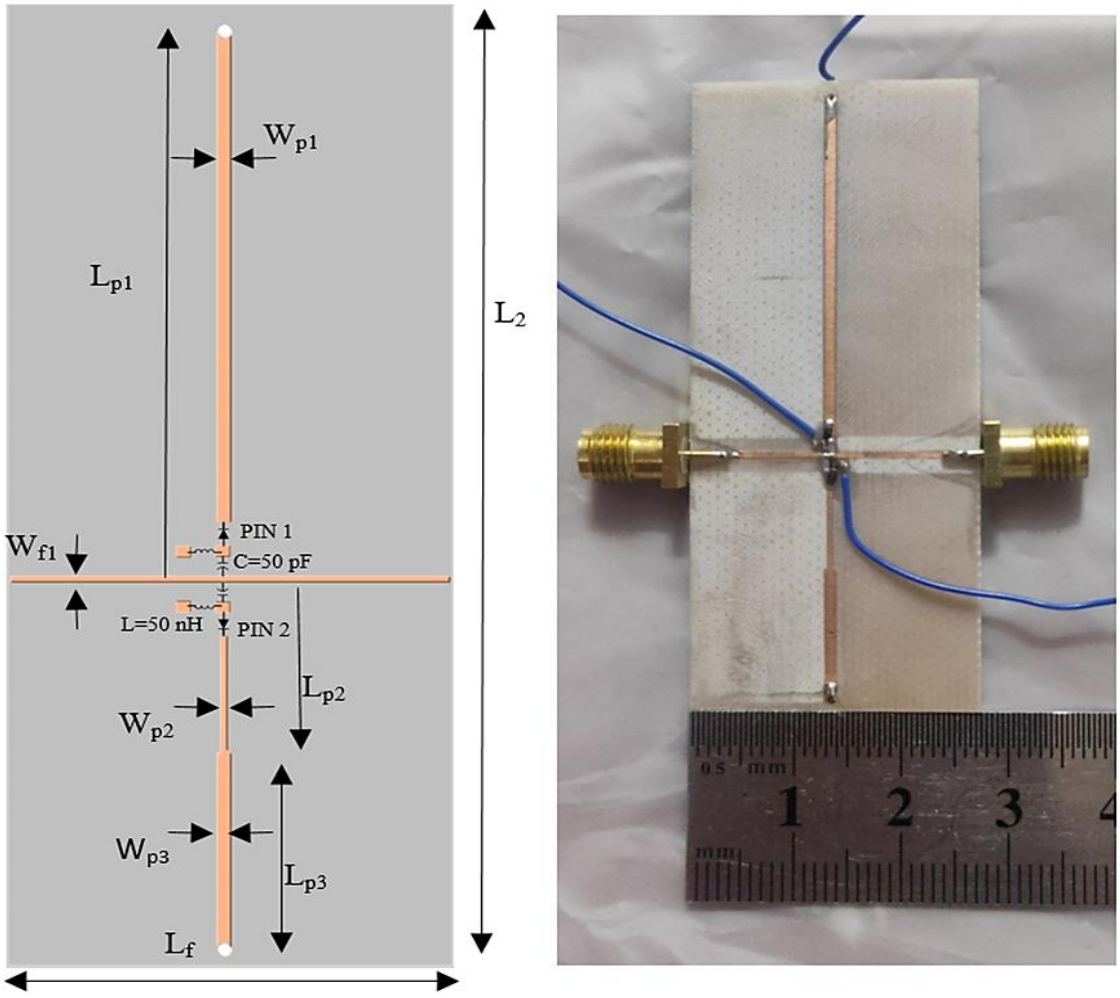

Figure 6: Photograph and layout diagram of fabricated microstrip bandstop filter with dual reconfigurable stubs utilizing SMP-1430-079 PIN diodes (design no. 2)

Moreover, Figure 6 serves as a visual representation of the filter's architecture and offers a comprehensive visualization of the input impedance (Z_{in}) of the presented filter across a spectrum of frequencies, further improving the understanding of its dynamic behavior. The resonators constituting the design experienced a precise and detailed photographic etching procedure, after which they were exactly assembled to give rise to an integrated circuit. This methodical assembly process is creatively depicted in Figure 5, providing a visual narrative of the intricate stages of bringing together the individual components to form the unified circuit.

Table 8: Geometrical dimensions overview for the reconfigurable dual bandstop filter (design no. 2)

Parameters	**h**	**L_2**	**L_{p1}**	**L_{p2}**	**L_{p3}**	**L_f**	**W_{p1}**	**W_{p2}**	**W_{p3}**	**W_f**
Dimension (mm)	0.8	65	36.2	10.74	13.4	27.44	1	0.5	1	0.5

5. Results and discussion

The first design implemented the reconfigurability function by incorporating one SMP-1340-079 PIN diode. Integrating the DC biasing circuit is a crucial component, featuring a combination of a PIN diode alongside a 50 pF capacitor, serving as DC blocks, and a 50 nH inductor, functioning as an RF choke. The PIN switch is characterized by a series resistance of 1 Ω for the ON condition as shown in Figure 7 (a). Conversely, specific parameters in the OFF-condition PIN switch include a junction resistance of 100 kΩ and a capacitance of 0.3 pF as illustrated in Figure 7 (b). Table 9 comprehensively explains the effective PIN states incorporated into this designed filter. Meanwhile, Figure 5 visually describes the positioning of the PIN diodes. The schematic diagram of the presented reconfigurable bandstop filter (Design No. 1) illustrates the placement of the DC biasing circuit with the PIN diode.

Table 9: Switching State of the Presented Microstrip Bandstop Filter with Reconfigurable Stub (Design No. 1)

No.	**Switch States**	**Filter state**	**Stop bands (GHz)**	**B.W (%)**	**S_{11} (-dB)**	**S_{21} (-dB)**
1	ON	BSF	2.4	23	0.7	27
2	OFF	non	-	-	-	-

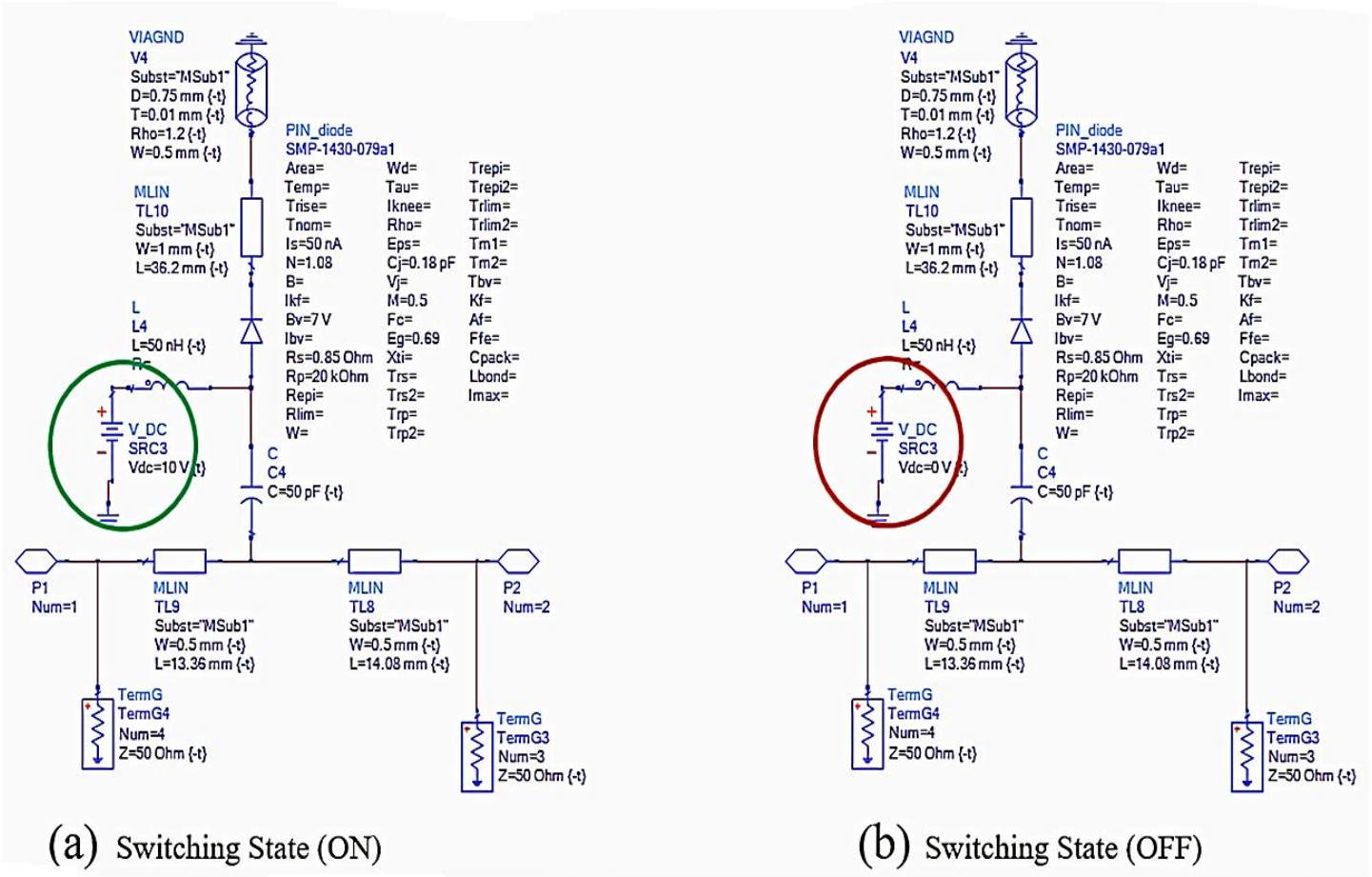

Figure 7: Applying the reconfigurability function to the microstrip bandstop filter with reconfigurable stub (design no. 1) (a) ON state (b) OFF state

Analyzing the simulated responses of S_{11} and S_{21} for the proposed reconfigurable bandstop filter in switching state No. 1 shows the process of the bandstop frequency at 2.4 GHz with a fractional bandwidth of 23%. This operation also exhibits S_{11} and S_{21} with approximately 0.7 dB and 27 dB, respectively. Notably, the filter shows a remarkable band-pass in 1.9 and 3.4 GHz. There are no remarkable results after transitioning to switching state No. 2, where the PIN diode is simulated to disconnect the feedline and resonator, maintaining other physical dimensions, as illustrated in Figure 5. It is essential to highlight that the primary objective of this design is to assess the impacts of the reconfiguring elements. The focus remains on understanding the influence of the PIN diode in altering the filter's performance characteristics. Figure 8 provides a visual representation of the simulation responses for S_{11} and S_{21} for the reconfigurable bandstop filter in this particular state. Figure 8 (a) represent the ON state result while Figure 8 (b) present the OFF state result This graphical description enhances our understanding of the dynamic changes induced by the reconfiguring elements, contributing to a more detailed investigation of the filter's behavior in response to switching states.

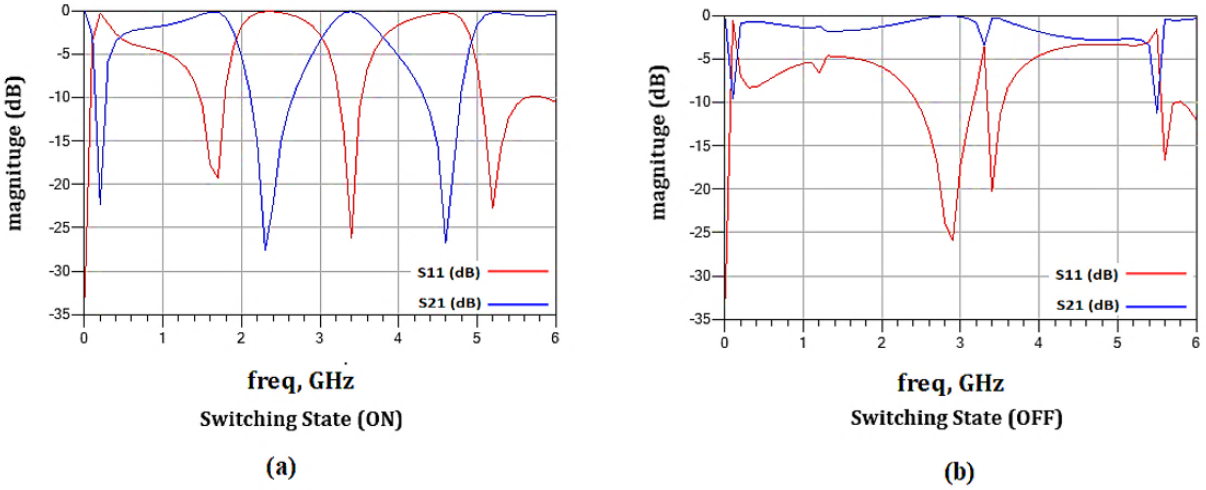

Figure 8: Simulated result of microstrip bandstop filter with reconfigurable stub (design no. 1) (a) ON state (b) OFF state

According to the above results, it becomes evident that the filter's skirt selectivity can be enhanced by integrating two transmission peaks. The first transmission peak is established within the low-frequency band, exactly at T_{PL} = 1.9 GHz, giving a magnitude of 0.5 dB. At the same time, the second transmission peak shows at the high-frequency band, precisely at T_{PH} = 3.4 GHz, with a magnitude of 0.6 dB. Furthermore, another stop band raises at 4.6 GHz. Using the Agilent/Keysight N9923A Vector Network Analyzer (VNA), the manufactured filter is carefully tested, and the attained results are studied through comparative assessment with the simulated results shown in Figure 8. To confirm the practical efficiency of the studied reconfigurable filter, Figure 9 and Figure 10 display the features of the S_{11} and S_{21} parameters related to the presented reconfigurable stop-band filter.

As shown in Figure 9 (a and b), an alignment between practical and simulation results is noticeable. However, a notable observation affects the filter's insertion loss, possibly due to the conventional manufacturing process. The noted frequency shift in practical results from substrate impurities, as depicted in Figure 10 (a and b). Examining the simulation outcomes shows a single passband at 560 MHz within the frequency of 2.4 GHz. The filter circuit's dimensions are 27.44 mm × 41 mm, notably at 0.54 λg × 0.8 λg (where λg is derived at 2.4 GHz), excluding the 50-ohm feeding stubs, showing the precision and specificity required in the design. Continuous advancements in fabrication techniques and material technologies hold promise for justifying these challenges, raising the evolution of future filter designs.

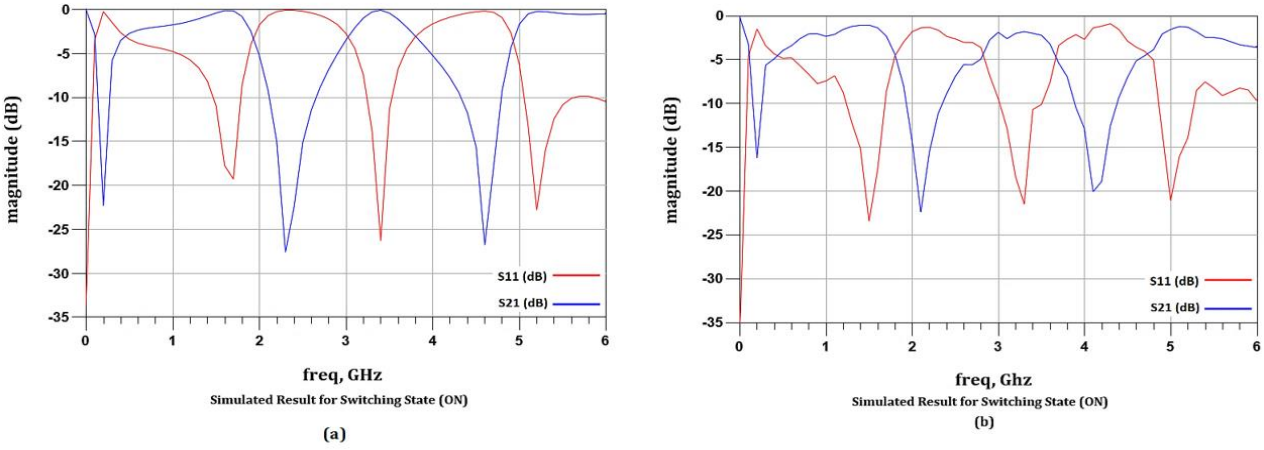

Figure 9: Measured and simulated result of microstrip bandstop filter with reconfigurable stub (design no. 1) (a) simulated result (b) measured result

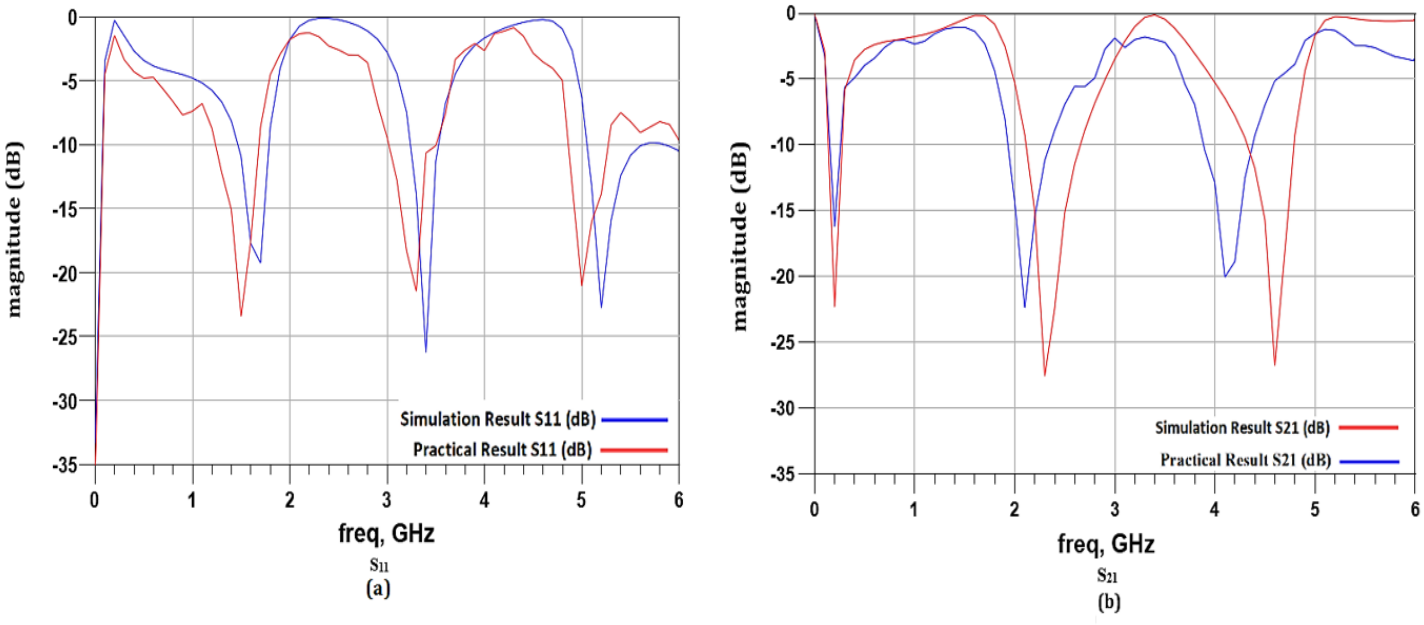

Figure 10: Comparison between the measured and simulated results of bandstop reconfigurable filter (design no. 1) (a) S_{21} response (b) S_{11} response

At the same time, the SMV1231 varactor tuning element is used to tune the operating frequencies with capacitance value extended from 0.466 to 2.35 pF depending on bias voltage range from 15 to 0 V. Figure 11 (b) illustrates the simulation results for S_{11} and S_{21} of the reconfigurable bandstop filter with the controlling of the varactor tuning, while Figure 11 (a) the schematic diagram of the presented reconfigurable bandstop filter (Design No. 1) with the varactor switch, providing to a complete estimation of the filter's performance in the presence of PIN and varactor diodes separately.

For the Second presented reconfigurable dual-band stop filter, the application of the reconfigurability function involves the utilization of two SMP-1340-079 PIN diodes in the proposed design. Integrating the DC biasing circuit is a fundamental consideration, combining a PIN diode, a 50 pF capacitor, serving as DC blocks, and a 50 nH inductor, functioning as an RF choke. Table 10 provides a comprehensive summary, showing the effective PIN states integral to this filter design. Simultaneously, Figure 12 (a-d) visually illustrates the positioning of the PIN diodes, offering a graphical representation of their strategic placement within the overall filter configuration. Analyzing the simulated responses of S_{21} and S_{11} for the proposed dual-bandstop filter in switching state No. 1 shows the achievement of the 1st bandstop frequency at 2.4 GHz and the 2nd operating frequency at 3.5 GHz, each with a fractional bandwidth of 23% and 16%, respectively. The filter displays S_{11} and S_{21}, evaluating at approximately 0.7 dB/30 dB and 0.6 dB/29 dB for the first and the second stop bands, respectively. This result also shows an excellent band pass, covering 1.85 GHz, 2.9 GHz, and 3.9 GHz.

Moving to switch state No. 2, where the PIN diodes are operated for a single bandstop filter at 2.4 GHz, the simulation performance of S_{11} and S_{21} is 0.8 dB/23 dB, respectively.

Similarly, the stop-band filter presents a fractional bandwidth of 28%. The stop-band features of this state offer effective pass bands at adjacent frequencies, precisely at 1.8 GHz and 3.3 GHz.Switching state No. 3 shows the PIN diodes simulated for a single bandstop filter at 3.5 GHz, while the simulation responses S_{11} and S_{21} exhibit 0.8 dB / 23 dB. Correspondingly, the stop-band filter in this state offers a fractional bandwidth of 3.5 GHz, equal to 17%. The stop-band performance is notable, effectively passing the nearby frequencies at 2.4 and 4.2 GHz. No remarkable results need to be discussed in switching state No. 4, where the PIN diodes are replaced by a disconnection between the feedline and resonator, maintaining other physical dimensions, as illustrated in Figure 6. Figure 13 visually describes the simulation responses S_{21} and S_{11} for the reconfigurable bandstop filter in these states, contributing to a more comprehensive understanding of the filter's behavior in the presence of PIN diode influence.

The selectivity of the designed filter was improved by incorporating three distinct maximum transmission frequencies. The initial transmission peak materializes within the low-frequency band, precisely positioned at T_{PL}=1.8 GHz, showcasing a magnitude of 0.7 dB. Concurrently, the second transmission peak emerges in the mid-frequency band, specifically at T_{PM}=2.9 GHz, with a magnitude of 0.7 dB, adding to the nuanced selectivity of the filter response. Also, the third transmission peak becomes discernible within the high-frequency band, occurring at T_{PH}=4 GHz and exhibiting a magnitude of 0.8 dB. Additionally, it is noteworthy that the rejection band extends beyond 5 GHz, highlighting the extensive range over which the filter effectively attenuates undesired frequencies. Once again, the testing procedure is directed at the fabricated filter by employing the Agilent/Keysight N9923A Vector Network Analyzer (VNA). The resultant measurements are subjected to a comparative analysis against the simulated results, as shown in Figure 13 (a-d). The S_{11} and S_{21} parameters of the proposed reconfigurable dual stop-band reconfigurable filter are described in Figures 14 and 15 to validate the practical results.

Table 10: Switching state of the offered microstrip bandstop filter with dual reconfigurable stubs utilizing PIN diodes (design no. 2)

No.	Switch States	Filter state	Stop bands (GHz)	B.W (%)	S_{11} (-dB)	S_{21} (-dB)
1	ON-ON	BSF	2.4, 3.5	23, 16	0.7, 0.6	30, 29
2	ON-OFF	BSF	2.4	28	0.8	23
3	OFF-ON	BSF	3.5	17	0.8	23
4	OFF-OFF	non	-	-	-	-

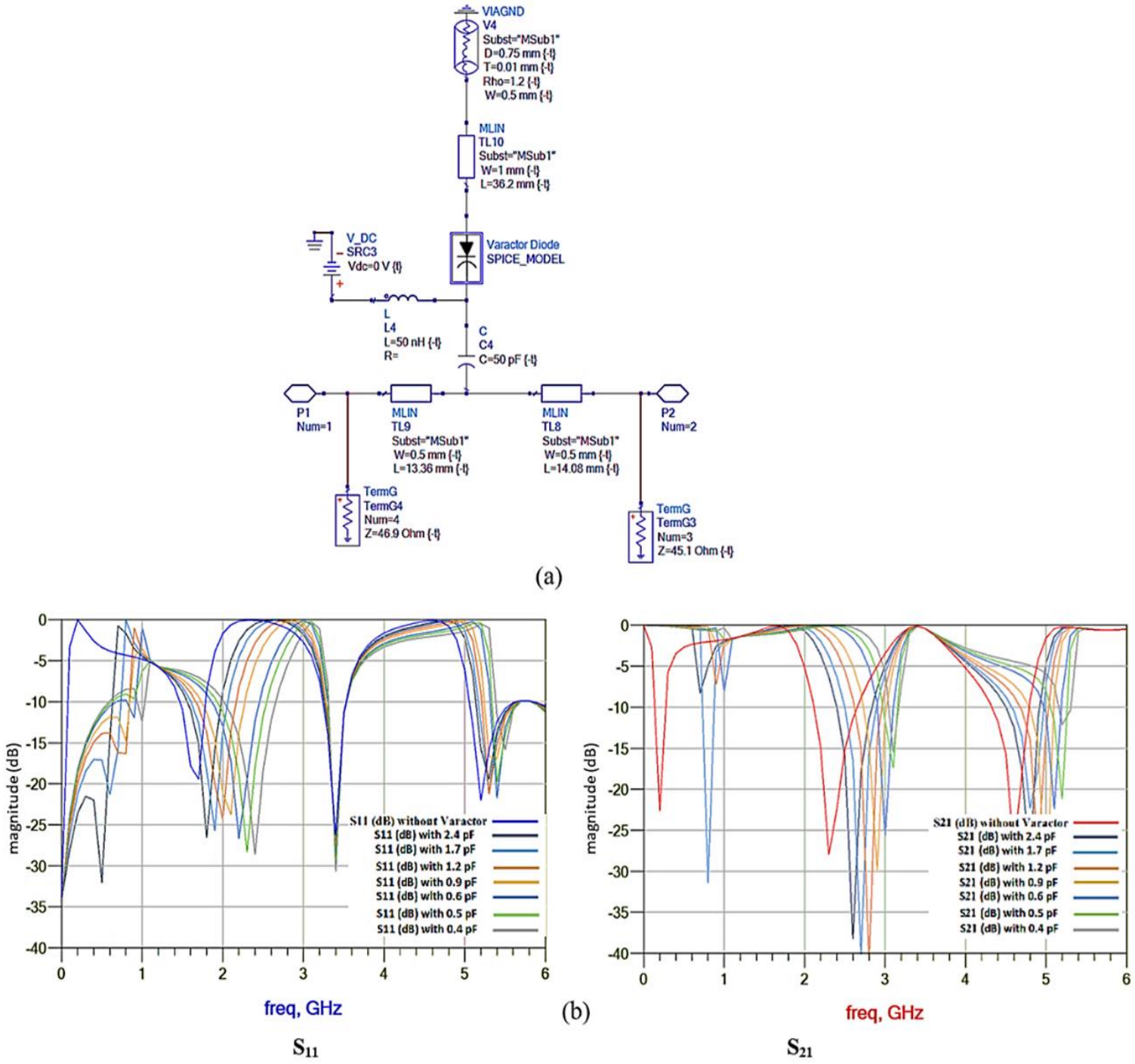

Figure 11: Microstrip bandstop filter with tunable stub (design No. 1) (a) schematic diagram (b) simulated results

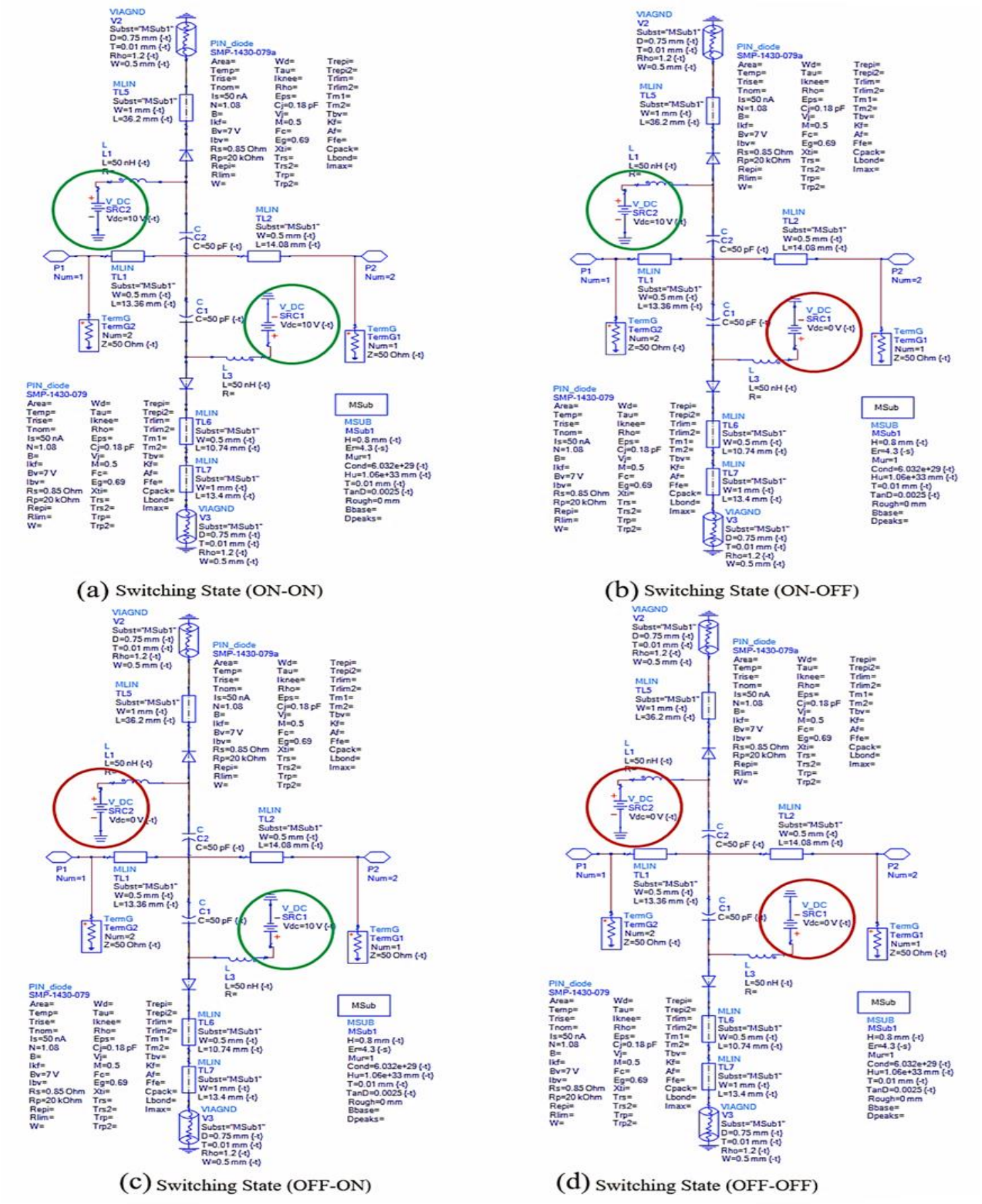

Figure 12: Applying the reconfigurability function to the microstrip bandstop filter with dual reconfigurable stubs utilizing PIN diodes (design no. 2) (a) ON-ON state (b) ON-OFF state (c) OFF-ON state (d) OFF-OFF state

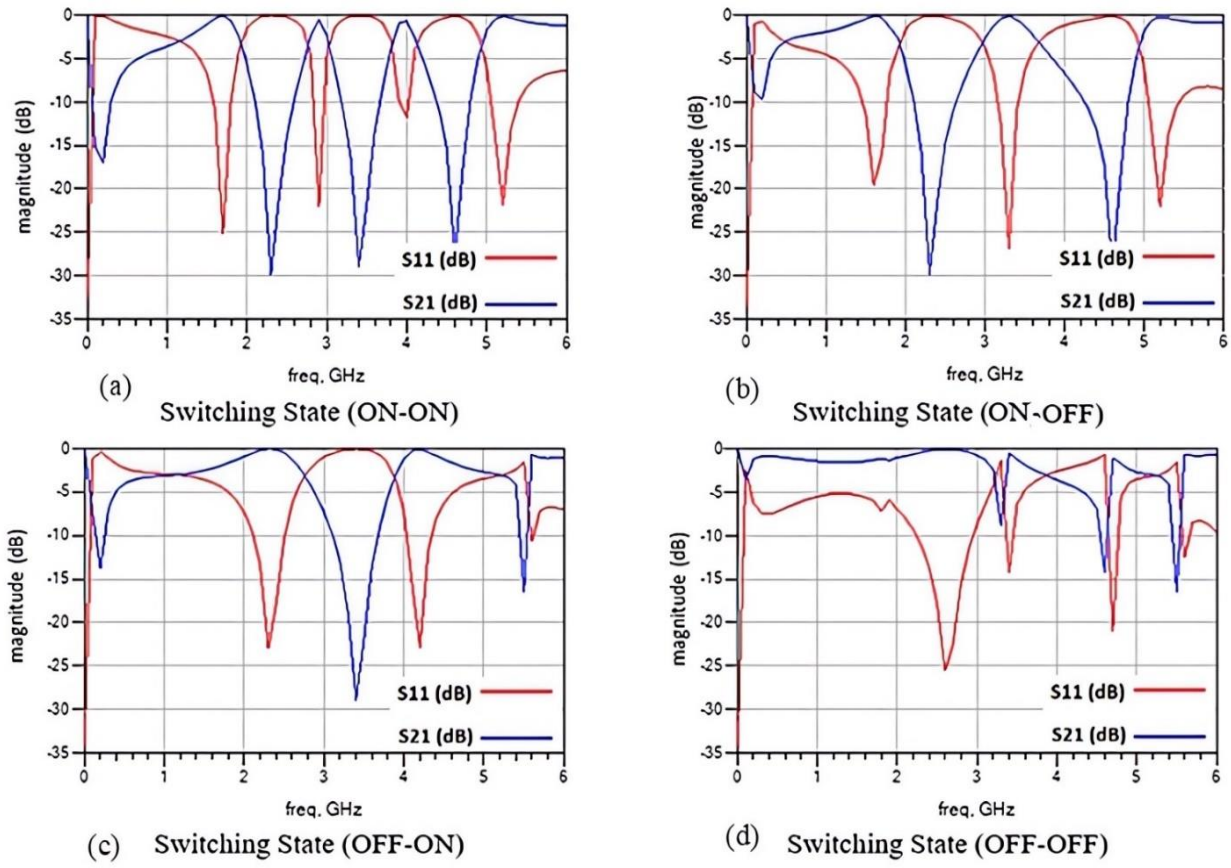

Figure 13: Simulated result of microstrip bandstop filter with dual reconfigurable stubs utilizing PIN diodes (design no. 2) (a) ON-ON state (b) ON-OFF state (c) OFF-ON state (d) OFF-OFF state

As illustrated in Figure 14 (a-f), a noticeable convergence between practical and simulation results is apparent. Nevertheless, the observed insertion loss in the filter can be assigned to utilizing a traditional manufacturing process. A notable detail is the frequency shift observed in practical results, a phenomenon arising from substrate material impurities, as outlined in Figure 15 (a-f). Examining simulation outcomes reveals the filter's appearance of two distinct stop-bands, specifically at 480 MHz / 2.4 GHz and 460 MHz / 3.5 GHz. This filter exhibits pass bands at frequencies 1.85 GHz, 2.9 GHz, and 3.9 GHz, respectively. The dimension of the filter circuit is 27.44 mm × 65 mm, particularly at 0.54 λg × 0.96 λg, excluding the 50-Ω feeding stubs. The presented filters were compared with previous related research, as illustrated in Table 11, and related to other proposed filters.

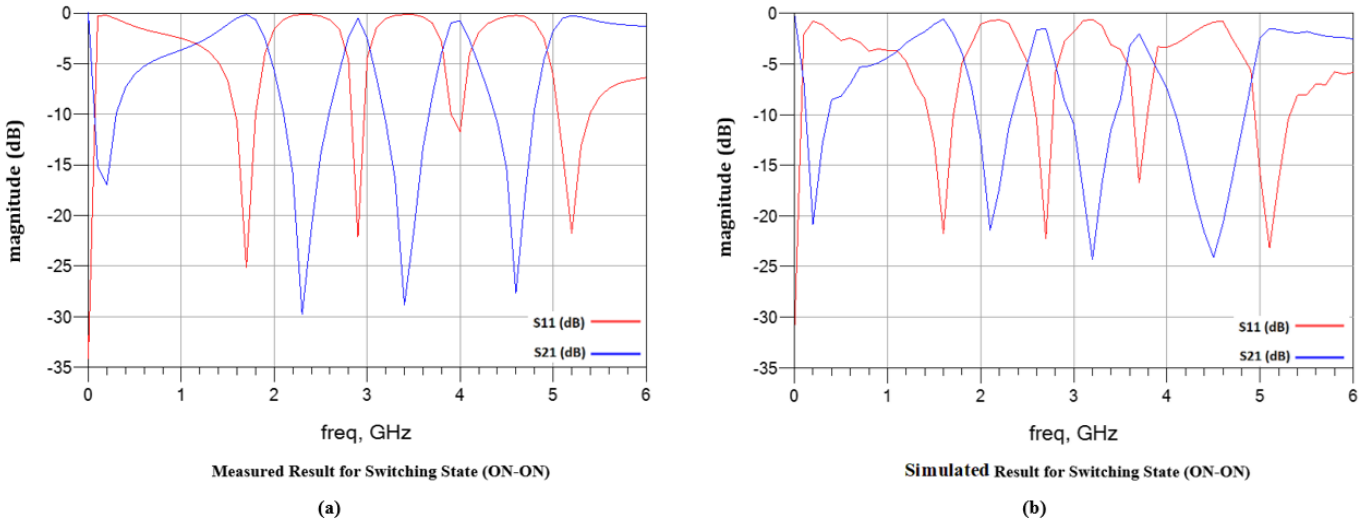

Figure 14: Measured and simulated result of microstrip bandstop filter with dual reconfigurable stubs utilizing PIN diodes (design no. 2) (a) simulated result for ON-ON state (b) measured result for ON-ON state (c) simulated result for ON-OFF state (d) measured (b) result for ON-OFF state (e) simulated result for OFF-ON state (f) measured result for OFF-ON state

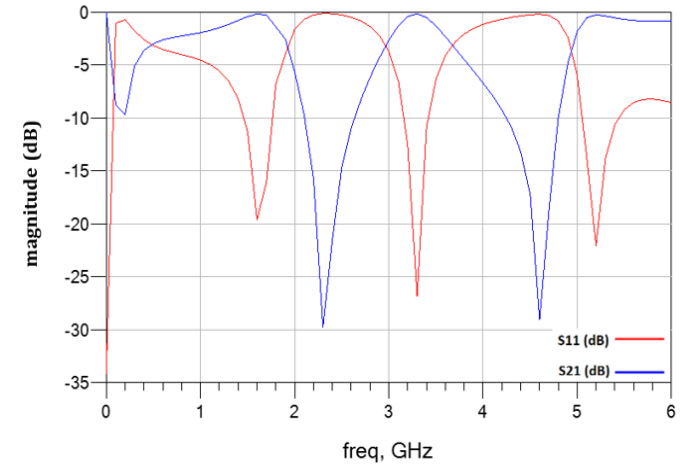

Measured Result for Switching State (ON - OFF)

(c)

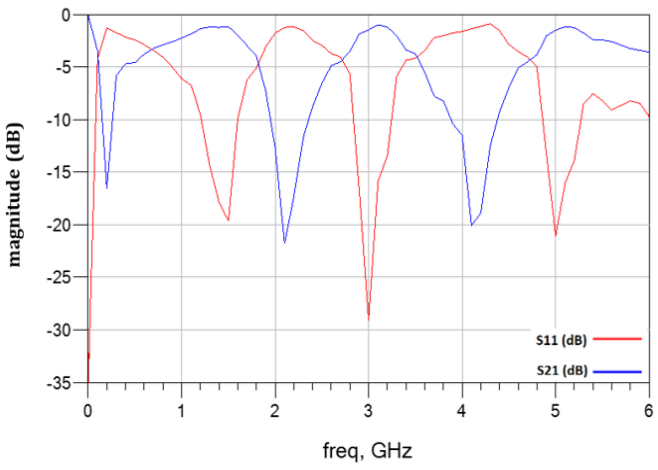

Simulated Result for Switching State (ON - OFF)

(d)

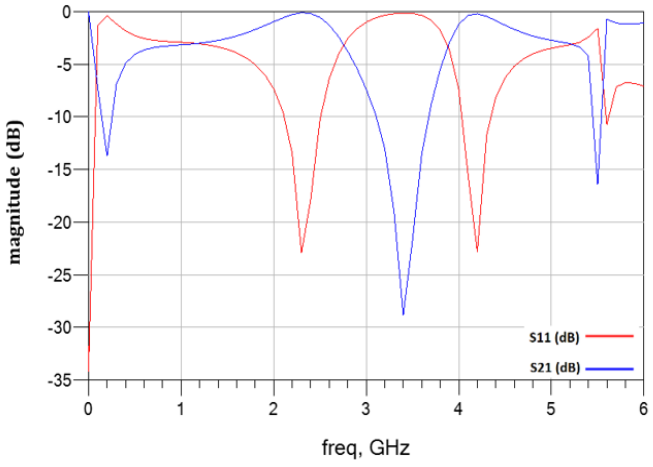

Measured Result for Switching State (OFF - ON)

(e)

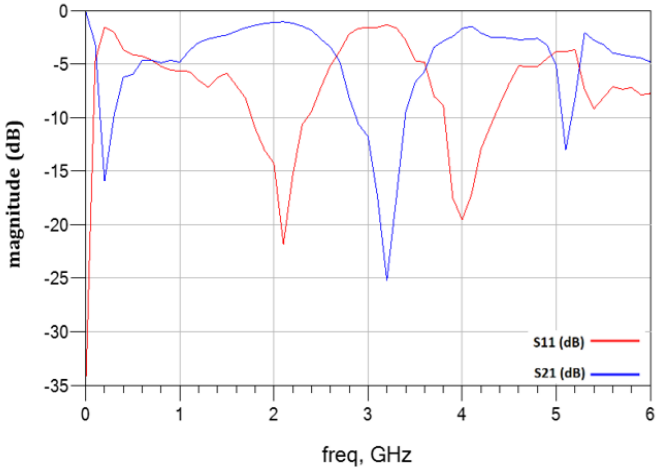

Simulated Result for Switching State (OFF - ON)

(f)

Figure 14: Continued

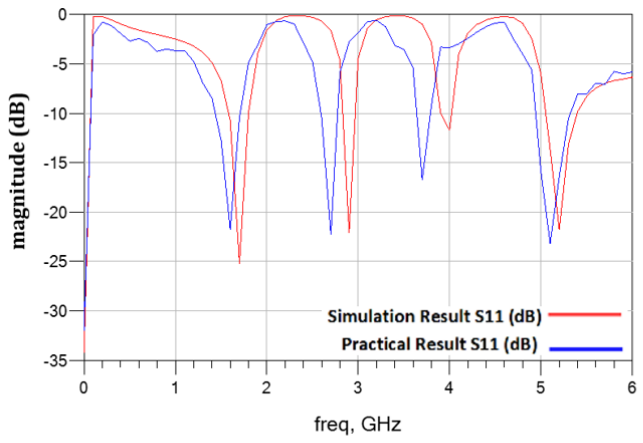

S_{11}

(a)

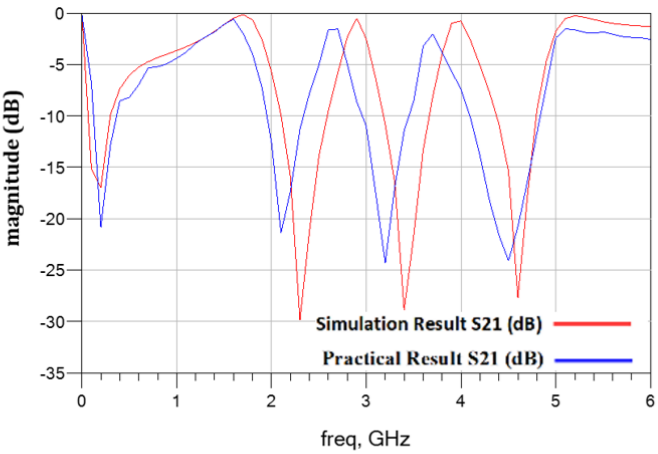

S_{21}

(b)

Measured and Simulated Result for Switching State (ON-ON)

Figure 15: Comparison between the measured and simulated results of bandstop reconfigurable filter (design no. 2) (a) S11response measured and simulated results for ON-ON state (b) S21 response measured and simulated results for ON-ON state (c) response measured and simulated results for ON-OFF state (d) S21 response measured and simulated results for ON-OFF state (e) S11 response measured and simulated results for OFF-ON state (f) S21response measured and simulated results for OFF-ON state

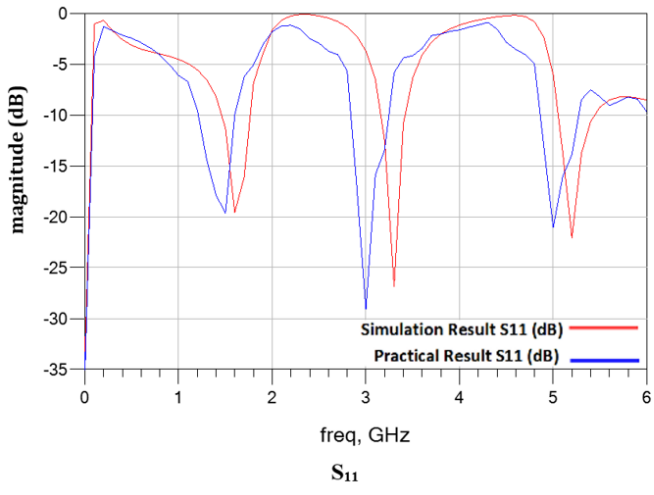

S_{11}

(c)

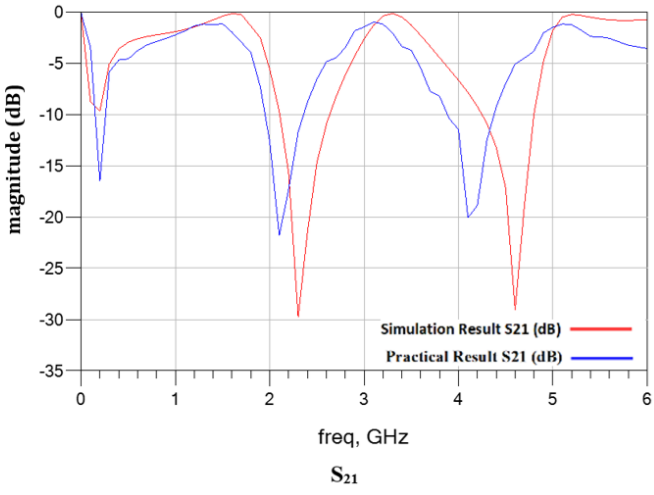

S_{21}

(d)

Measured and Simulated Result for Switching State (ON-OFF)

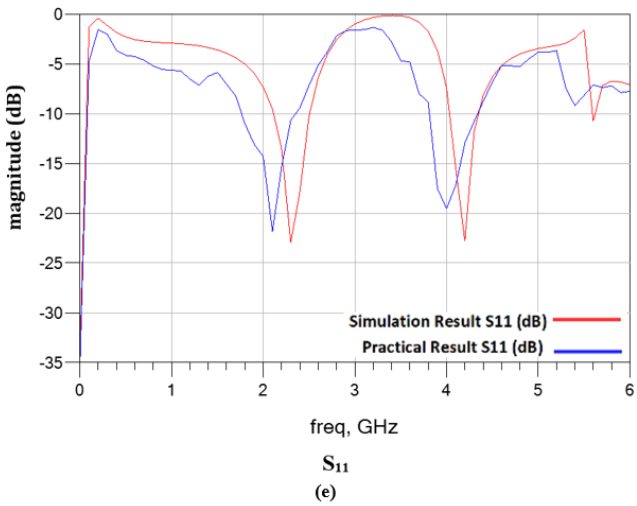

S_{11}

(e)

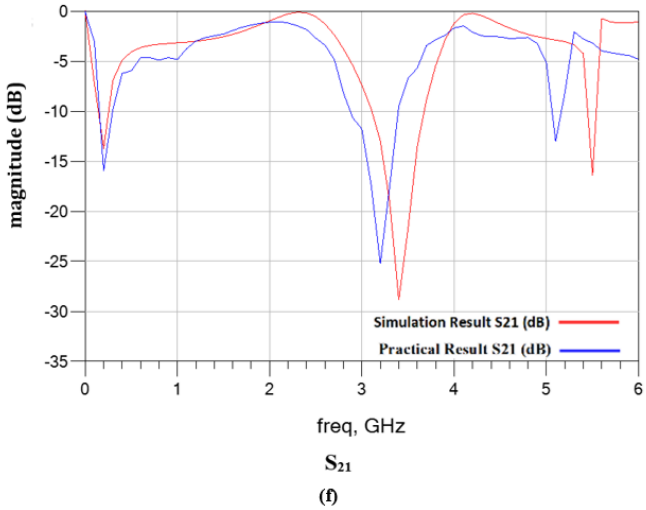

S_{21}

(f)

Measured and Simulated Result for Switching State (OFF-ON)

Figure 15: Continued

Table 11: Comparison with recently reported topologies

Bandpass (GHz)	B.W (%)	S_{11} (−dB)	S_{21} (−dB)	Circuit size ($\lambda_g \times \lambda_g$)	No. of reconfiguring elements	Ref.
8.5 – 14, 9 – 15.5	47.82, 54.16	20, 30	1.6, 1.2	0.9 × 0.96	4	[3]
3.6	55	20	0.6	0.2 × 0.22	7	[4]
0 – 1, 3.4 – 3.8	100, 11	30	1.4	0.4 × 0.32	1	[5]
1.5, 1.6	7	23, 18	1.3, 2.3	0.27 × 0.12	2	[6]
5, 10	70	50, 30	2.6, 2.1	0.32 × 0.35	2	[7]
1.3 - 3.2, 6.5 - 7.5	84, 8	42, 35	0.9, 0.6	0.45 × 0.45	2	[8]
2.4	42	20	1.2	0.52 × 0.67	3	[13]
0.6 - 2	17, 13	34	0.6	0.75 × 0.98	9	[14]
8.327 - 13.942, 4.62 - 6.2	51, 29	32	0.6	0.66 × 0.66	4	[15]
1.24-1.64, 1.4-1.6	28, 13	42, 40	1.3, 1.7	0.59 × 0.96	4	[16]
0.8 – 1.95	12, 83	20	1.3	0.23 × 0.14	3	[17]
2, 3	27, 13	22	1.5	0.52 × 0.67	6	[18]
0.5, 1.2	6, 11	34	2.6	0.17 × 0.27	3	[19]
1.8, 3.4	22, 6	24, 21	1.6, 2.5	0.54 × 0.8	1	Design No.1
2.4 (stop band freq.)	23 (for stop band)	2 (for stop band)	23 (for stop band)			
1.85, 2.9, 3.9	11, 4, 5	22, 23, 16	0.9, 2, 2.4	0.54 × 0.96	2	Design No.2
2.4, 3.5 (stop band freq.)	20, 13 (for stop band)	1, 0.9 (for stop band)	21, 25 (for stop band)			

6. Conclusion

This article provides a comprehensive analysis of reconfigurable filter design, concentrating on the impact of varactors and PIN diode switches, in combination with capacitors and inductors, on the filter response. The study's objectives are to classify reconfigurable filters according to their functions in the reconfigurability process and the use of reconfiguring components.

Investigating the essential parameters like frequency tuning and bandwidth alteration, the research further discovers the effect of these reconfigurable components on insertion and return losses, offering a complete understanding of their use in filter design. The study compares the theoretical and practical testing to confirm the proposed theories supported by the two presented bandstop filter (BSF) designs. The first reconfigurable bandstop filter design comprises a single stub resonator set to work at a frequency of 2.4 GHz. The second reconfigurable dual-mode filter operates with two separate frequencies, "f_{odd}" at 3.5 GHz and "f_{even}" at 2.4 GHz. These filters were implemented using the SMP-1340-079 PIN diode. Incorporating a DC biasing circuit with a PIN diode, a capacitor of 50 pF as DC blocks, and an inductor of 50 nH as an RF choke are involved in attaining the reconfigurability purpose. The presented filters include functions with acceptable results. However, the offered reconfigurable filters encounter difficulties in practical operation caused by fabrication limitations.

Author contributions

Conceptualization, **S. Mahdi**, **M. Raheema**, and **R. Hammed**; data curation, **S. Mahdi**, **M. Raheema**, and **R. Hammed**; formal analysis, **S. Mahdi**, **M. Raheema**, and **R. Hammed**; investigation, **S. Mahdi**, **M. Raheema**, and **R. Hammed**; methodology, **S. Mahdi**, **M. Raheema**, and **R. Hammed**; resources, **S. Mahdi**, **M. Raheema**, and **R. Hammed**; software, **S. Mahdi**, and **R. Hammed**; supervision, **M. Raheema**, and **R. Hammed**; validation, **S. Mahdi**, **M. Raheema**, and **R. Hammed**; visualization, **S. Mahdi**, **M. Raheema**, and **R. Hammed**; writing—original draft preparation, **S. Mahdi**, and **M. Raheema**; writing—review and editing, **S. Mahdi**, and **M. Raheema**. All authors have read and agreed to the published version of the manuscript.

Funding

This research received no specific grant from any funding agency in the public, commercial, or not-for-profit sectors.

Data availability statement

The data that support the findings of this study are available on request from the corresponding author.

Conflicts of interest

The authors declare that there is no conflict of interest.

References

[1] Z. QinLi, Z. Ren, P. Liu, L. Liao, X. Qiu and Z. Li, Varactor based continuously tunable microstrip band-pass filters: A review, issues and future trends, IEEE Access, 12 (2024) 157443 - 57457. https://doi.org/10.1109/access.2024.3383788

[2] H. Islam, S. Das, T. Bose and T. Ali, Diode based reconfigurable microwave filters for cognitive radio applications: A review, IEEE Access, 8 (2020) 185429–185444. https://doi.org/10.1109/access.2020.3030020

[3] M. Alqaisy, V. Chakrabraty, K. Ali, V. Alhawari and T. Saeidi, Switchable square ring band-pass to bandstop filter for ultra-wideband applications, Int. J. Microwave Wireless Technolog., 9 (2015) 51–60. https://doi.org/10.1017/s1759078715001373

[4] M. A. Abdalla, D. K. Choudhary and R. K. A. Chaudhary, Compact reconfigurable band-pass/low-pass filter with independent transmission zeros based on generalized Nri metamaterial, Int. J. RF Microwave Comput. Aided Eng., 30 (2019). https://doi.org/10.1002/mmce.22074

[5] Y. Al-Yasir, Y. Tu, N. Ojaroudi Parchin, A. Abdulkhaleq, J. Kosha, W. Mshwat, E. Elfoghi, H. Migdadi and R. Abd-Alhameed, Novel and very compact reconfigurable band-pass to low-pass/band-pass microstrip filter with wide-stopband restriction for 5G communications, Proc.1st International Multi-Disciplinary Conf. Theme: Sustainable Development and Smart Planning, IMDC-SDSP 2020, Cyperspace, 28-30 June 2020. https://doi.org/10.4108/eai.28-6-2020.2298131

[6] S. Kingsly, M. Kanagasabai, M. G. Alsath, S. Subbaraj, S. K. Palaniswamy and B. Bhuvaneswari, Switchable resonator based reconfigurable band-pass / bandstop microstrip filter, Int. J. Electron., 108 (2021) 1610–1622. https://doi.org/10.1080/00207217.2021.1908613

[7] R. Allanic, F. L. Borgne, H. Bouazzaoui, D. L. Berre, C. Quendo, D. S. De Vasconcellos, V. Grimal, D. Valente and J. Billoué, On-Chip Bandstop to Band-pass reconfigurable filters using semiconductor Distributed doped areas (SCDDAs). Electronics, 11 (2022) 3420. https://doi.org/10.3390/electronics11203420

[8] T. Mehul, R. P. Pravin and S. Hitesh, Reconfigurable Dual Wide-band Bandstop- Band-pass Switching Filter Using PIN Diodes, Int. J. Microwave Opt. Technol., 18 (2023) 417–426.

[9] Y. Li, W. Li and Q. Ye, ,A reconfigurable triple-notch-band antenna integrated with defected microstrip structure band-stop filter for ultra-wideband cognitive radio applications, Int. J. Antennas Propag., (2013) 1–13. https://doi.org/10.1155/2013/472645

[10] J. Cui, A. Zhang, Z. Wu and S. Yan, A frequency reconfigurable filtering antenna based on stepped impedance resonator, J. Electromagn. Waves Appl., 34 (2020) 571–580. https://doi.org/10.1080/09205071.2020.1719212

[11] H. S. Syed, S. Anusuya, S. Susmitha, R. Srilalitha, S. Subasree and S.Vigneshwar, Design of Reconfigurable Wide Band Pass Filter, Int. J. Future Gener. Commun. Networking, 13 (2020) 1376–1382.

[12] A. Bandyopadhyay, P. Sarkar, T. Mondal and R. Ghatak, A dual function reconfigurable band-pass filter for wide-band and tri-band operations, IEEE Trans. Circuits Syst. II Express Briefs, 68 (2021) 1892–1896. https://doi.org/10.1109/tcsii.2020.3047873

[13] Y. Deng and K. Wu, Generalized synthesis method for Tunable and reconfigurable filter with flexible frequency response characteristics', XXXIth URSI General Assembly and Scientific Symposium (URSI GASS), 2014. https://doi.org/10.1109/ursigass.2014.6929373

[14] R. Gómez-García and A. C. Guyette, Reconfigurable multiband microwave filters, IEEE Trans. Microwave Theory Tech., 63 (2015) 1294–1307. https://doi.org/10.1109/tmtt.2015.2405066

[15] M. A. Alqaisy, C. Chakrabraty, J. Ali, A. R. Alhawari and T. Saeidi, Reconfigurable bandwidth and tunable dual-band Band-pass filter design for Ultra-Wideband (UWB) applications, Electromagnetics, 36 (2016) 366–378. https://doi.org/10.1080/02726343.2016.1207766

[16] D. Simpson, R. Gómez-García, D. Psychovisual, Single-/multi-band band-pass filters and duplexers with fully reconfigurable Transfer-Function characteristics, IEEE Trans. Microwave Theory Tech., 67 (2019) 1854–1869. https://doi.org/10.1109/tmtt.2019.2899849

[17] M. Fan, K. Song, Y. Fan, Reconfigurable band-pass filter with wide-range bandwidth and frequency control, IEEE Trans. Circuits Syst. II Express Briefs, 68 (2021) 1758–1762. https://doi.org/10.1109/tcsii.2020.3040190

[18] S. Kingsly, M. Kanagasabai, M. G. Alsath, P. S. Kumar, T. R. Rao, K. Indhumathi, S. Subbaraj and Y. P. Selvam, Compact frequency and bandwidth reconfigurable microwave filter, Wireless Pers. Commun., 115 (2020) 1755–1768. https://doi.org/10.1007/s11277-020-07652-0

[19] X. Chen, T. Yang, P. Chi, Novel single-ended-to-balanced filter with reconfigurable working modes, frequency, bandwidth, and Single/Dual-Band operations, IEEE Access, 9 (2021) 14216–14227. https://doi.org/10.1109/access.2021.3051312

[20] H. Nachouane, A. Najid, A. Tribak, F. Riouc, A switchable bandstop-to-bandpass reconfigurable filter for cognitive radio applications, Int. J. Microwave Wireless Technolog., 9 (2016) 765–772. https://doi.org/10.1017/s175907871600074x

[21] C. D. Manikya Krishna, Reconfigurable Hairpin Band-pass Filter for Wireless Applications, Int. J. Eng. Technol., 7 (2018) 229–232.

[22] M. Potrebić, D. Tošić, and A. Plazinić, Reconfigurable multilayer dual-mode band-pass filter based on memristive switch. AEU - Int. J. Electron. Commun., 97 (2018) 290–298. https://doi.org/10.1016/j.aeue.2018.10.032

[23] S. Kingsly, M. Kanagasabai, G. N. Mohammed, S. Subbaraj, Y. Panneer Selvam and R. Natarajan, Multi-band reconfigurable microwave filter using dual concentric resonators, Int. J. RF Microwave Comput. Aided Eng., 28 (2018). https://doi.org/10.1002/mmce.21290

[24] S. Triapthi, N. P. Pathak, and M. Parida, A compact reconfigurable multi-mode resonator-based multiband band pass filter for intelligent transportation systems applications, Def. Sci. J., 68 (2018) 547. https://doi.org/10.14429/dsj.68.12769

[25] F. Zhang, Y. Gao, Y. Wang, Y. Zhang, Y. and J. Xu, A compact tri-band microstrip filter with independently tunable passbands and high selectivity, IEICE Electron. Express, 16 (2019) 20190589–20190589. https://doi.org/10.1587/elex.16.20190589

[26] D. Borah, T. S. Kalkur, Reconfigurable balanced Dualband bandstop filter, International applied computational electromagnetics society symposium (ACES), 2020. https://doi.org/10.23919/aces49320.2020.9196042

[27] S. Yang, W. Li, M. Vaseem and A. Shamim, Fully printed VO_2 switch based flexible and reconfigurable filter, 2020 IEEE/MTT-S International Microwave Symposium (IMS), 2020. https://doi.org/10.1109/ims30576.2020.9224095

[28] X. -K. Bi, X. Zhang, S.-W. Wong, S.-H. Guo and T. Yuan, Reconfigurable-bandwidth DWB BPF with fixed operation frequency and controllable stop-band, IEEE Trans. Circuits Syst. II Express Briefs, 68 (2021) 141–145. https://doi.org/10.1109/tcsii.2020.3001872

[29] F. Wei, C. Y. Zhang, C. Zeng and X. W. Shi, A reconfigurable balanced Dual-Band Band-pass filter with constant absolute bandwidth and high selectivity, IEEE Trans. Microwave Theory Tech., 69 (2021) 4029–4040. https://doi.org/10.1109/tmtt.2021.3093907

[30] D. R. Kumar ,C. B. Rajshekhar, Reconfigurable interdigital band-pass filter for wireless applications, Turk. J. Comput. Math. Educ., 12 (2021) 2704–2710. https://doi.org/10.17762/turcomat.v12i12.7917

[31] H. Boubakar, M, Abri and M. Benaissa, Design of complementary hexagonal metamaterial based HMSIW band-pass filter and reconfigurable SIW filter using PIN diodes, Adv. Electromagn., 10 (2021) 19–26. https://doi.org/10.7716/aem.v10i2.1596

[32] H. Boubakar, M. Abri and M. BenaïSsa, Electronically reconfigurable HM-SIW band-Pass filter based on new CSRR design using PIN diodes, J. Inf. Math. Sci., 13 (2021), 59–69. https://doi.org/10.26713/jims.v13i1.1567

[33] J. Lai, T. Yang, P. Chi,R. Xu,1.866–2.782-GHz reconfigurable filtering Single-Pole-Multithrow switches based on Evanescent-Mode cavity resonators, IEEE Trans. Microwave Theory Tech., 69 (2021) 1355–1364. https://doi.org/10.1109/tmtt.2020.3039960

[34] M. E. Gomaa, A. A. Abd-El-Hadi and Esmat, compact reconfigurable triple bandstop filter using defected microstrip structure (DMS), Prog. Electromagn. Res., C, 136 (2023) 13–22. http://dx.doi.org/10.2528/PIERC23051808

[35] J. Cheng and Y. Li, A reconfigurable multiband resonator and its application to band-pass filter, J. Phys. Conf. Ser., 2578 (2023) 012035. https://doi.org/10.1088/1742-6596/2578/1/012035

[36] M. Smari, S. Dakhli, E. Fourn and F. Choubani, Reconfigurable Bandstop Filter with Switchable CLLs for Bandwidth Control, Prog. Electromagn. Res. Lett., 110 (2023) 11–19. https://doi.org/10.2528/pierl23022206

[37] P. Vryonides, S. Nikolaou, S. Kim and M. M. Tentzeris, Reconfigurable dual-mode band-pass filter with switchable bandwidth using PIN diodes, Int. J. Microw. Wirel. Technol., 7 (2014) 655–660. https://doi.org/10.1017/s1759078714000932

[38] K. Devi, K. Umadevz , and J. Baligar, Reconfigurable compact band-pass microstrip filter of bandwidth 1.54ghz, Am. J. Networks Commun., 8 (2019) 59. https://doi.org/10.11648/j.ajnc.20190802.12

[39] Y. I. Al-Yasir, N. O. Parchin, Y. Tu, A. M. Abdulkhaleq, I. T. Elfergani, J. Rodriguez andR. A. Abd-Alhameed, A varactor-based very compact tunable filter with wide tuning range for 4G and sub-6 GHz 5G Communications, Sensors, 20 (2020) 4538. https://doi.org/10.3390/s20164538

[40] H.M. Al-Tamimi, S. Mahdi, A Study of Reconfigurable Multiband Antenna for Wireless Application, Int. J. New Technol. Res., 2 (2016) 125-134

[41] Advanced design system (ADS), (2017), Electromagnetic, Santa Rosa, CA 95403-1738, United States: Agilent Technologies.

[42] R. T. Hammed, Miniaturized dual-band bandstop filter using multilayered e-shape microstrip structure, Eng.Technol. J., 34 (2016) 2096–2105. https://doi.org/10.30684/etj.34.11a.15

[43] H. I. Khani , A. S. Ezzulddin, A survey on microstrip single/multiband band-pass filter for 5G applications, Eng. Technol. J., 41 (2024) 467- 483. https://doi.org/10.30684/etj.2022.135858.1288